Nordic nuclear safety research

NKS-393
ISBN 978-87-7893-481-9

Modelling of a Large Water Pool during Operation of Blowdown Pipes, Spargers, and Nozzles

Ignacio Gallego-Marcos, Walter Villanueva, Pavel Kudinov

Division of Nuclear Power Safety
Royal Institute of Technology (KTH)
Sweden

August 2017

Abstract

In a Boiling Water Reactor, steam released from primary coolant system is condensed in the pressure suppression pool. Thermal stratification in the pool affects pressure suppression capacity of the pool. Heat and momentum sources generated by the steam condensation define pool behavior. Direct Contact Condensation (DCC) of steam present a challenge for contemporary modeling tools. In previous work, the Effective Heat Source (EHS) and Effective Momentum Source (EMS) models were proposed to simulate development of thermal stratification or mixing induced by steam injection into a large pool of water. These models are computationally efficient and sufficiently accurate in resolving the effect of DCC phenomena on the large scale pool circulation.

EHS/EMS models for blowdown pipes have been extended to predict the transition between condensation regimes, estimate the effective momentum of chugging, allow capturing non-uniform condensation along the pipe, and modelling the drywell and wetwell during prototypic LOCA conditions. Validation against the POOLEX-MIX 04 experiment shows very good agreement with the pool temperature and containment pressure.

In the spargers, the experimental data has been analyzed to identify the most important physical phenomena to be considered in the CFD modelling. Based on this analysis, EHS/EMS models for spargers have been developed and implemented in ANSYS Fluent, and validated against the PANDA HP5-1 and 2 experiments. Comparison to pool temperature shows good agreement with the model predictions.

Key words

Thermal Stratification, Mixing, Pressure Suppression Pool, Spargers, Mixing Nozzles, Containment, Thermal Hydraulic, GOTHIC, BWR

NKS-393
ISBN 978-87-7893-481-9
Electronic report, August 2017
NKS Secretariat
P.O. Box 49
DK - 4000 Roskilde, Denmark
Phone +45 4677 4041
www.nks.org
e-mail nks@nks.org

Modelling of a Large Water Pool during Operation of Blowdown Pipes, Spargers, and Nozzles

Final Report from the NKS-R COPSAR activity (Contract: NKS_R_2015_114)

Ignacio Gallego-Marcos, Walter Villanueva, Pavel Kudinov

Royal Institute of Technology (KTH),
Roslagstullsbacken 21, 10691
Stockholm, Sweden

June 2017

EXECUTIVE SUMMARY

The development of thermal stratification in the pressure suppression pool of boiling water reactors (BWRs) and in-containment refueling water storage tanks (IRWST) of advanced pressurized water reactors (PWRs) is an issue of safety significance. Pools stratification can (i) affect the operation of the spray and Emergency Core Cooling System (ECCS) that use the pool as a source of water, and (ii) lead to higher containment pressures. The main systems affecting thermal stratification or mixing of the pool are spargers, mixing nozzles, blowdown pipes, and sprays. Validated models are necessary for prediction of the pool and containment performance during an accident.

Lumped and 1D codes are missing adequate models for simulation of 3D phenomena in the pool, such as transient mixing and stratification. Application of CFD is too computationally expensive for modeling of realistic plant accident scenarios. The Effective Heat Source (EHS) and Effective Momentum Source (EMS) models were developed as middle ground approach which provides (i) computational efficiency, and (ii) sufficient accuracy in resolving the safety important phenomena and parameters. The EHS/EMS predict the time and space averaged effect of the small scale direct contact condensation phenomena on the large scale circulation and heat transfer in the pool. Athe concept of the EHS/EMS models has been developed and validated previously for blowdown pipes for flow chugging and internal condensation regimes. In this work, we present further development and validation of the EHS/EMS models for blowdown pipes, sparger, and mixing nozzles.

For the blowdown pipes, correlations have been developed to predict the transition between condensation regimes, and to estimate the effective momentum of chugging. These correlations are function of the steam mas flux, pool sub-cooling, and geometry of the injection system. They were built using the PPOOLEX and all other all available experimental data. A new implementation of the EHS/EMS models in GOTHIC has been proposed to enable simulating the pool and containment behavior during prototypic LOCA conditions. A time-averaging model has also been proposed to minimize the effect of the numerical oscillations on the pool behavior. Validation against the PPOOLEX MIX-04 experiment shows very good agreement to the pool temperatures and containment pressure.

A scaling methodology has been developed and applied to the sparger and mixing nozzle experiments performed in PPOOLEX and PANDA. The goal was to preserve prototypical ranges of injection conditions and pool regimes occurring during prototypical BWR transients. The data obtained with the scaled experiments was used for analysis of the physical phenomena and code validation. Important physical phenomena to be considered in the CFD modelling has been identified: for example, the erosion and mixing mechanisms of the stratified layer, the oscillations of the thermocline interface, the self-similarity of the liquid jets induced by the sparger, and the downwards inclination of the jets. Codes and EHS/EMS models validated for these conditions can be then used to predict plant behavior.

The EHS/EMS models for spargers are under development. An experimental setup to measure the effective momentum induced by the oscillatory bubble regime during a steam injection through spargers has been designed by LUT with support from KTH.

The EHS/EMS models for spargers have been implemented in ANSYS Fluent. It has been shown that using the k-Omega BSL turbulence model with the SGDH and a $C_{3\varepsilon}$ varying between 0 and 1 allows a good prediction of the stable stratification and erosion regimes. Validation of the EHS/EMS implementation in Fluent against the PANDA HP5-1, 2 experiments shows good agreement with the experimental data.

Keywords: Thermal Stratification, Mixing, Pressure Suppression Pool, Spargers, Mixing Nozzles, Containment, Thermal Hydraulic, GOTHIC, BWR.

Table of contents

1. INTRODUCTION

Boiling Water Reactors (BWR) are the second most common models of nuclear reactors. Compared with Pressurized Water Reactors (PWR), BWRs are built with a much smaller containment gas space since they do not need to accommodate the steam generators used in PWRs. This lower volume poses a risk in Loss-Of-Coolant Accident (LOCA) scenarios, where large flow rates released into the containment can cause very fast pressurizations. To avoid this issue, BWRs rely on the Pressure Suppression Pool (PSP), a large water pool where steam is passively injected and condensed [1]. The large volume of the PSP allows storing large quantities of decay heat, making it a valuable system for other long-term transients such as Station Black Outs (SBO). It also serves as a water source for the Emergency Core Cooling System (ECCS), spray, and as a scrubber for the possible radioactive elements escaping from the core. Advanced PWR models such as the AP1000, APR1400, and EPR are designed with a similar pool, known as the In-containment Refuelling Water Storage Tank (IRWST) [2].

In a BWR, steam can be injected into the pool through blowdown pipes and spargers [3]. The first connect the drywell to the wetwell, inject steam vertically downwards, and are typically used during a LOCA. Spargers connect the primary circuit to the wetwell, inject steam radially through a multi-hole head, and are used during a SBO to regulate the pressure in the primary circuit. In Nordic BWRs, nozzles are also used to inject a high momentum liquid flow into the pool which could mix the pool, preventing the development of thermal stratification.

Direct condensation of steam injected into a water pool is as a source of heat and momentum. Competition between these sources determines whether the pool is thermally stratified or mixed [4, 5]. For example, if steam is injected at low momentum, the latent heat is deposited in the water layer above the pipe outlet, while water below the pipe outlet remains cold. The small momentum induced by the flow of condensed liquid at the pipe outlet can be insufficient to overcome buoyancy forces that support the stability of the hot layer [6, 7]. Steam injections at higher momentum (e.g. chugging, oscillatory bubbles, and stable jets) can create larger momentum sources, and lead to development of a large scale circulation in the pool which can break or erode the stratified layer [6, 7].

The development of thermal stratification in the PSP is an issue of safety significance. Steam condensation is very limited if the water temperature at the pipe outlet is close to saturation, even if bottom layer of the pool remains cold. Thus, stratification limits steam condensation capacity of the pool. Moreover, the pool surface temperature determines the steam partial pressure in the containment gas space. Higher surface temperatures of a stratified pool will lead to higher containment pressure compared to a completely mixed pool, at the same average pool temperature. For instance, the containment pressure was rapidly increasing at Fukushima Daiichi Unit 3 during first 12 hours of the operation of the Reactor Core Isolation Condenser (RCIC) [8, 9]. When the pressure reached 400 kPa, the automatic protection system had to shut down the RCIC, leaving the plant without core makeup water. Based on mixed pool assumption, lumped parameter codes under-estimated the maximum pressure by about 160 kPa [8]. Higher pressure was attributed to the development thermal stratification in the suppression pool.

Modelling the pool behavior during a steam injection is a challenge due to the direct contact condensation phenomena. While CFD is too computationally expensive [10, 11, 12], lumped and 1D codes are inadequate for prediction of 3D, transient mixing phenomena. In general, state-of-the-art approaches cannot capture the effect of different condensation regimes due to the lack of the physical models. In this work, we present the development and validation of the Effective Heat Source and Effective Momentum Source (EHS/EMS) models [4, 5, 13] for blowdown pipes and sparger. The main idea of these models is that, to predict the global pool behavior, direct contact condensation phenomena occurring at the small temporal and spatial scales do not need to be resolved. Instead, it is the time-averaged Effective Heat (EHS) and Momentum (EMS) Sources transferred from the steam to the large scale pool circulation what needs to be modelled.

In this work, the status of the goals and tasks of the project are presented in Section 2. Section 3 provides a state of the art review of the work done on direct contact condensation and pool behavior. Sections 4 defines the EHS/EMS models, and Sections 5, 6, and 7 the specific development for blowdown pipes, sparger, and mixing nozzles.

2. GOALS AND TASKS

The main goal of the project is to develop, validate and apply modelling capabilities for assessment of the PSP performance in Nordic BWR containments. In order to achieve the goal of the project, the main research objectives are: to develop and validate modelling capabilities of condensation, heat transfer and mixing in pressure suppression pools. In the Roadmap 3 for 2014-2018, developed by NORTHNET, following high priority tasks were identified as necessary to achieve the ultimate goal of the project:

- Task-1: To develop EHS/EMS models for the blowdown pipes in case of different steam condensation regimes and presence of non-condensable gases.
- Task-2: To develop EHS/EMS models for spargers and RHR nozzles.
- Task-3: To provide analytical support for PSP tests in the Nordic BWRs.
- Task-4: To validate the EHS/EMS models against OECD/HYMERES PANDA tests.
- Task-5: To provide analytical support to NORTHNET partners in addressing containment performance.
- Task-6: Analytical support for PPOOLEX tests and GOTHIC validation.

In the framework of the NKS COPSAR project main goals of KTH work were to perform pre-test analysis and simulations for selection of operational regimes and test procedures, and post-test analysis and validation with EHS/EMS models implemented in GOTHIC against PPOOLEX tests with (i) RHR nozzles, (ii) spargers; further development and validation of the EHS/EMS models for spargers and RHR nozzles against respective separate effect tests.

This report summarizes main results obtained in the framework of NKS COPSAR and NORTHNET RM3 projects and begins with an introduction and formulation of respective goals and tasks and brief overview of the tasks' status in Sections 1 and 2. State-of-the-art and literature review of previous works done in direct contact condensation and pool behavior is presented in Section 3. The status of the Effective Heat Source and Effective Momentum Source model (EHS/EMS) developed for blowdown pipes and spargers are presented in Sections 5 and 6 respectively.

2.1. Status of the Tasks

2.1.1. Task-1: To improve EHS/EMS models for the blowdown pipes.

In case of LOCA steam injection into pressure suppression pool is provided through blowdown pipes. Different LOCA scenarios (large, medium, small) will result in different regimes of steam condensation in the pool. These regimes can affect development of stratification or mixing of the pool.

This task aims to continue the development of the EHS/EMS models for the blowdown pipes in order to reduce their uncertainties and to improve their predictive capabilities and accuracy. In particular, it improves implementation of the EHS/EMS models for the prediction of:

- Effective heat flux distribution inside blowdown pipe in case of different condensation regimes.
- Frequency and amplitude of oscillations in the blowdown pipe using scaled experimental data and analytical models.
- Effect of non-condensable gases and steam escaping from the pipe outlet on the effective heat source.

The task also includes validation of developed models against already available data and new experiments.

The work is motivated by the results of POOLEX and PPOOLEX tests which suggest that stratification characteristics in the upper layer of the pool depend on the regime of condensation inside the blowdown pipe. In addition, the original models developed by Nariai for prediction of condensation oscillations have rather large uncertainty when applied to larger scale (e.g. PPOOLEX) tests.

Specific goals for this task are:

- To develop modifications of the EHS model for non-uniform condensation in the blowdown pipe. This will help to improve accuracy in prediction of temperature distribution in the stratified layer. The modified model for non-uniform condensation can be validated against PPOOLEX test data.
- To develop for EMS detailed maps for the effective momentum induced by the oscillations in the blwodown pipe. Existing analytical models for prediction of the frequency and amplitude were developed using data from small scale experiments at limited range of parameters. Proper extension of the models to larger scale experiments and prototypic plant conditions is necessary.
- To modify EMS model in order to take into account contribution to the effective momentum of non-condensable gases, and steam flowing from the pipe to the pool. These effects are important for the clearing phase of small and medium LOCA and also for relatively large steam flux at low sub-cooling of water in the pool. Validation of the modified model for non-condensable gases will be contingent upon the availability of relevant experimental data from LUT.

Status of Task-1

New correlations have been developed to predict the transition between condensation regimes, and to estimate the effective momentum of chugging. These correlations were obtained as functions of the steam mas flux, pool sub-cooling, and geometry of the injection system using the PPOOLEX and other available experimental data. A new implementation of the EHS/EMS models in GOTHIC has been proposed to enable simulating the pool and containment behavior during prototypic LOCA conditions. A time-averaging model has also been proposed to minimize the effect of the numerical oscillations of the flow in the pool. Validation against the PPOOLEX MIX-04 experiment shows very good agreement to the pool temperatures and containment pressure. For more details, see paper *"Modelling of a Steam Blowdown into the Pressure Suppression Pool of a BWR during a LOCA Using GOTHIC"* (Submitted to Journal: Annals of Nuclear Energy).

2.1.2. Task-2: To develop EHS/EMS models for spargers and RHR nozzles.

Main motivation for the Task 2 is necessity to have a complete set of models for simulation of the most important components in the pressure suppression pool. Development, implementation and validation of EHS/EMS for steam injection through spargers of SRVs and nozzles of RHR are necessary for the analysis of plant transients. It is planned to modify the PPOOLEX, i.e. to change blowdown pipe to a realistic sparger design. This should then be combined by development and verification of a scaling methodology allowing interpretation of PPOOLEX data using validated codes in prediction of full scale PSP conditions.

Specific goals for this task are:

- To develop necessary models to simulate dynamics of the pool mixing and stratification in case of steam injection through spargers and mixing by the RHR pumps, and

- To validate the models against separate effect tests.

The EHS/EMS models should take into account the fact that momentum is created in a different steam condensation regime, that is, injection is through small multiple holes directed radially, and there are no large scale oscillations of steam-water interface.

For the pool mixing by nozzles of RHR pumps, the idea is to develop a “subgrid modeling” approach in GOTHIC in order to take into account the effect of the small jet on the flow structure in the pool trying to avoid of resolving unimportant details of the flow in the close vicinity of the jet nozzle. Similar to blowdown pipes and spargers, the characteristic length scale of the RHR nozzle is orders of magnitude smaller than the characteristic length scale of the pool. Also, an accurate spatial resolution of the near nozzle jet region (CFD-like approach) is computationally expensive. Basically we are interested in prediction of large scale flow structure in the pool, which is responsible for mixing of stratified layer.

Status of Task-2

An experimental setup to measure the effective momentum induced by the oscillatory bubble regime during a steam injection through spargers has been designed by KTH and LUT. Preliminary experiments are expected to be performed before the end of the year, and continued through 2018. The experimental data will be used to analyze the physical phenomena affecting the oscillatory bubble regime, and to develop theoretical models which can predict the effective momentum.

A series of tests with mixing nozzles has been carried out at LUT. The validation of the models against the data is ongoing.

2.1.3. Task-3: To provide analytical support for PSP tests in the Nordic BWRs.

Specific goals for this task are:

- Development and verification of a scaling methodology allowing interpretation of both data from both PPOOLEX and full scale PSP tests using validated codes in prediction.
- Development realistic plant containment models for simulation of the PSP transients.
- Validation of the code and models against test data.
- To propose test conditions for the future experiments and to provide pre-test analysis.

Status of Task-3

A scaling methodology has been developed and applied to design the sparger and mixing nozzle experiments performed in PPOOLEX and PANDA facilities. The goal was to preserve prototypical ranges of injection conditions and pool regimes occurring during prototypical BWR transients. The data obtained with the scaled experiments was used for analysis of the physical phenomena and code validation. Important physical phenomena to be considered in the CFD modelling has been identified: for example, the erosion and mixing mechanisms of the stratified layer, the oscillations at the thermocline, the self-similarity of the liquid jets induced by the sparger, and the downwards inclination of the jets. Codes and EHS/EMS models validated for these conditions can be then used to predict plant behavior. Specific transients to be addressed in the plant scale are under evaluation.

For more details, see paper: *"Sparger Experiments on Thermal Stratification and Mixing Performed in the PPOOLEX and PANDA Facilities"* (To be submitted in Journal: International Journal of Heat and Mass Transfer).

2.1.4. Task-4: To validate the EHS/EMS models against PANDA tests.

The goals for this task are:

- To provide analytical support for pre-test analysis of the experiments in OECD/HYMERES research program and post-tests validation of the codes.
- To validate EHS/EMS against PANDA data.
- To validate GOTHIC against data from complex transient with injection of steam and non-condensable gases into the PSP and into the drywell, taking into account the effects of cooling and steam condensation in the gas phase, possible activation of vacuum breakers, etc.

Validation of GOTHIC code prediction against PANDA facility at PSI, Switzerland is a unique possibility to enhance understanding of the effect of the scales.

More detailed description of the tasks for this part of the project are:

- to identify the most important relevant phenomena to be addressed in the test series;
- to develop PANDA facility input models for GOTHIC and validate them against previous PANDA tests;
- to participate in the OECD/NEA-PSI CFD Benchmark for blind validation of the input models;
- to provide pre-test analysis in order to determine specific conditions of the tests;
- to suggest the test matrix which would address the phenomena including the effects of cooling and steam condensation in the gas phase, possible activation of vacuum breakers, etc.;
- to carry our post-test validation of GOTHIC and developed by KTH models against PANDA data.

Status of Task-4

The EHS/EMS models for sparger have been implemented in ANSYS Fluent. It has been shown that using the k-Omega BSL turbulence model with the SGDH and a $C_{3\varepsilon}$ varying between 0 and 1 allows a good prediction of the stable stratification and erosion regimes. Validation of the EHS/EMS implementation in Fluent against the PANDA HP5-1, 2 experiments shows good agreement with the experimental data.

For more details, see papers:

- *"Modeling of Thermal Stratification and Mixing Induced by a Steam Injection Through Spargers into a Large Water Pool"* (Published in CFD4NRS-6, Boston, USA, 2016).
- *"Scaling and CFD Modelling of the Pool Experiments with Spargers Performed in the PANDA Facility"* (Published in NUTHOS-11, Gyeongju, Korea, 2016).

2.1.5. Task-5: To provide analytical support to NORTHNET partners in addressing containment performance.

The analytical support is provided with developed and validated tools in assessment of PSP related safety margins in uprated plants. A non-exhaustive list of the sub-tasks which can be addressed in the framework of this work includes:

- Pre- and post-test analytical support of possible future test in the plants.

- Analytical support in addressing containment performance issues where mixing and stratification both in liquid and in gas phase are important, e.g. steam-nitrogen mixing in the upper drywell and its influence on performance of filtered containment venting and hydrogen behavior in the containment, containment building, and in the filter system.
- Verification of consequences of operator actions in different accident scenarios.

Status of Task-5

Further development and validation of the EHS/EMS models will be done against available experimental data to confirm the current hypothesis and further improve the prediction capability. Modelling approaches which allow using the developed EHS/EMS models in coarse mesh models in GOTHIC will also be developed to enable sensitivity and uncertainty analysis of plant transients.

2.1.6. Task-6: Analytical support for PPOOLEX tests and GOTHIC validation.

The goals of this task are

- To provide analytical support for future PPOOLEX tests with pre-test analysis for selection of the operational regimes and test procedures.
- Post-test analysis and validation of GOTHIC code against experimental data.

This work will be tightly coupled with the experimental activities carried out at LUT on containment spray and possible PCCS tests. The need for improvement of GOTHIC models in prediction of these phenomena will be addressed based on the results of code validation

Status of Task-6

Analytical support has been provided to the PPOOLEX and PANDA experiments with spargers and mixing nozzles. Pre-test simulations were run using GOTHIC. In the mixing nozzle experiments, the experimental results were observed to be very similar to the pre-test predictions. Analytical support will also be given for the separate effect facility to be built in LUT. Post-test analysis of the EHS/EMS models implemented GOTHIC showed good agreement to the pool behavior during the sparger tests SPA T1, T3, T4, T7. In order to address concerns about possible effect of the code, ANSYS Fluent was also used for this purposes. Eventually, ANSYS Fluent, where the radial injection of the sparger can be better represented, was selected as the computational platform to validate the EHS/EMS models for spargers against the PANDA tests.

For more details, see NKS report

- Ignacio Gallego-Marcos, Walter Villanueva, Pavel Kudinov, "*Thermal Stratification and Mixing in a Large Pool Induced by Operation of Spargers, Nozzles, and Blowdown Pipes*," NKS research report, NKS-369, 2016.

3. STATE OF THE ART REVIEW

The pool behavior during a steam injection is governed by a large number of parameters. For example, direct contact condensation determines the heat and momentum sources injected into the pool, single phase flow the transport of these sources across the pool, and density interfaces the transport between the stratified layer and the rest of the pool. Experimental data allows us to identify the most important variables affecting these phenomena. Based on these variables, analytical and numerical models can be developed to predict the pool behavior.

This section we will begin by analyzing the experiments performed on direct contact condensation and pool behavior, sections 3.1 and 3.2 respectively, and conclude by presenting the numerical approaches used to model these phenomena, section 3.3.

3.1. Experiments on direct contact condensation

The steam condensation regimes which occur during an injection into a subcooled pool can be divided into two main groups: sonic, and sub-sonic. Sonic regimes occur when the injection pressure is about 0.53 times higher than the ambient one. The shear between vapor and liquid induces interface instabilities which entrain liquid droplets into the vapor core, leading to a highly diffused interface which gradually turns into a bubbly flow and eventually to single-phase liquid. Despite the unstable nature of the interface, sonic regimes are usually referred as “stable regimes”. This because the macroscopic jet parameters of penetration length, expansion ratio, heat transfer coefficient etc., remain relatively constant in time. Experiments performed in [14] show that the main variables affecting the aforementioned parameters are the steam mass flux, pool subcooling (saturation temperature minus pool temperature), and injection hole diameter. Thus, correlations of the jet parameters have been proposed as a function of these variables [14, 15, 16]. The shockwave pattern in sonic jets was studied by Wu et al. [17], where it is shown that high pressures after a shockwave cause an expansion of the jet when released into the pool. Since steam condensation is negligible during the expansion, the steam jet flow is confined to a divergent section which can accelerate to super-sonic conditions, leading to another shockwave. Successive contraction-expansion waves can occur depending on the pressure inside the sparger and in the pool.

The liquid jet induced by the steam condensation was investigated by Choo et al. [18] using Particle Image Velocimetry (PIV). It was concluded that the liquid turbulent jet becomes self-similar after a certain distance from the injection. Coefficients were also proposed to model the turbulent profile as a function of the injection conditions. Van Wissen et al. [19] measured the turbulent intensities induced in the liquid, which were observed to reach maximum values of 30 %.

In the sub-sonic regimes, the heat transfer between steam and liquid becomes lower than in sonic conditions [20]. Thus, jets are able to expand and generate bubbles which eventually detach and condense through a collapse [21, 22], giving the name of oscillatory bubble regime. The frequency of the bubble growth-detach-collapse cycle was analyzed by Fukuda [23], Hong et al. [24] and Cho et al. [25] for single and multi-hole injection respectively. The frequency was observed to vary between 50-600 Hz, and to depend mainly on the pool subcooling and injection hole diameter. For this regime, Tang et al. [26] studied the collapse mechanism of the detached bubbles and established a regime map. At lower steam mass fluxes, the flow enters into the chugging regime, where the collapse of large bubbles induces a sudden pressure drop which pushes liquid from the pool inside the injection pipe [27]. The transition between the oscillatory bubble and chugging regimes is characterized by a monotonic decrease of the detaching frequency along the steam mass flux range of 20-60 kg/(m^{2}s) [28], after which the frequency settles in stable values of 1-2 Hz [29]. Experiments performed by Aust & Seeliger [30] showed that chugging can be suppressed by designing a blowdown pipe outlet cut at 45^{o}. This effect was attributed to the counter-flow and high shear developing at the outlet section, which prevented large bubbles from forming for steam mass fluxes up to 100 kg/(m^{2}s).

At very low steam mass fluxes chugging is suppressed and all steam is condensed inside the blowdown pipe.

Single-hole condensation regime maps for sub-sonic regimes have been proposed by Aya & Nariai [31] Chan & Lee [21], Liang & Griffith [32], and Cho et al. [33]. In all of these works, the steam mass flux, pool and steam temperature were identified as the most important parameters determining the condensation regime. Petrovic de With et al. [34] combined the some of the previous maps into a 3D regime map which took into account the injection hole diameter. Condensation regime maps for the different modes of chugging regime were also proposed by Gregu et al. [35]. Multi-hole condensation regime maps for sonic and sub-sonic flow were proposed by [36], where it was observed that the transition between sonic and sub-sonic occurs at approximately 330 kg/(m^{2}s).

In a BWR, the pressure difference between the drywell and wetwell is determined by the submergence of the blowdown pipes, which can be between 1-6 m [1]. This hydro-static difference is usually not enough to trigger sonic flow. On the other hand, the large pressure difference between the primary circuit and the wetwell pool makes spargers more likely to inject steam in sonic regimes. This can occur during the intermittent operation of the Safety Relief Valves (SRVs), or at the initial stages of the Automatic Depressurization System (ADS). For LOCA, long-term ADS operations, or exhaust of safety systems such as the Reactor Core Isolation Condenser (RCIC), sub-sonic regimes are expected to dominate in the transient.

3.2. Experiments on pool behavior

The transport of the heat and momentum generated during a steam injection is affected by the geometry of the pool. The main variables are the total pool depth, which determines the strength of natural circulation; the submergence depth of the pipes, which determines the location of the stratified layer; and the cross section area, which determines the interaction of radial jets with the walls. Experiments are usually performed in reduced scale facilities, in comparison due to the prototypic scales of the pool in a BWR. In this case, adequate scaling becomes an essential ingredient for the design and interpretation of the test results [37].

The full-scale Marviken-FCSB tests performed in Sweden [38] showed that chugging occurs during prototypic LOCA transients in a BWR Mark II. Thermal stratification was also observed to develop once chugging was suppressed due to the reduction in the steam mass flux. Extensive experimental campaigns were carried out by General Electric in a 1:130 reduced scale facility to analyze the pool swelling, pressure increase, pool temperature, etc. during a LOCA in a BWR Mark I [39], Mark II [40, 41], and Mark III [42, 43, 44]. Unfortunately, these reports are not public. LOCA experiments were also performed in Japan by JAERI [45, 46] using a full scale 20^o sector of a BWR. Similar to Marviken, chugging was again present in most of the tests. However, since the duration of the JAERI experiments was limited to a few hundred seconds, no development of thermal stratification was observed.

The LINX facility [47] at Paul Scherrer Institut (PSI), Switzerland, was built to investigate the development of thermal stratification and mixing during the late stages (+1h) of a LOCA in a ESBWR. Steam was injected directly into the pool through a single-hole 40 mm vertical sparger. Air concentrations above 5% in mass were observed to cause a complete mixing of the pool; whereas pure steam led to a substantial thermal stratification development below the injection line, reaching temperature differences up to 30 ^{o}C [48]. Experiments performed by Moon et al. [49] focused on the high steam mass flux sonic regimes using prototypic multi-hole spargers of an APR1400. Due to the high jet momentum, complete mixing of the pool was observed in all of the tests. Experiments performed by Zhang et al. [50] with a scaled down models of the AP1000 quencher and IRWST showed that prototypic steam injection conditions can cause significant thermal stratification, specially due to the low submergence of the quenchers. Extensive experimental campaigns were performed in the POOLEX/PPOOLEX facility in Lappeenranta University of Technology (LUT), Finland, using blowdown pipes [51, 52, 53, 54, 55, 56]. Here, separate effect experiments were carried out to analyze the individual effect of parameters such as the drywell volume, pipe diameter, submergence, number of blowdown pipes, steam injection conditions, etc. Thermal stratification was observer during prototypic steam injection conditions of a BWR, even during weak chugging regimes.

Experiments in small scale facilities were performed by Solomon et al. [57], where it was observed that thermal stratification can develop during prototypic steam injections of the RCIC system. Experiments performed by Song et al. [58] confirmed that the pool Richardson number can be used to predicting the transition between thermal stratification and mixing.

Though some of the previous works were focused on the study of thermal stratification and mixing, little attention was given to the physical mechanisms which cause mixing and erosion of the stratified layer. In the field of atmospheric and oceanic research, Fernando [59] shows that the erosion regimes of stable stratified layer can be predicted by the bulk Richardson number. A detailed analysis done in by Fernando et al. [60, 61] further shows that low Richardson number flows are able to break down the stratified layer by penetrating into it. As the Richardson number increases, the turbulent eddies are only able to penetrate into the stratified layer, but only to impinge on it and splash some heavy liquid upwards. At very high Richardson numbers, turbulent eddies can only induce waves in the pool whose sporadic break up leads to local mixing. It has also been shown in [59] that the erosion velocity can be predicted as a function of the Richardson number and pool geometry.

3.3. Analytical and numerical modelling

Based on the experimental data presented in sections 3.1 and 3.2, a large number of works have been done in the modelling of direct contact condensation and pool behavior.

Analytical models to predict the bubble diameters and detachment frequency during the oscillatory bubble regime were developed in [62, 63] using the Rayleigh-Plesset equation and momentum balances across the bubble. Chugging models were also developed by Aya & Nariai [27] and Pitts [64] using the conservation equations. These works were later extended by [65] to include the presence of non-condensable gases. Comparison to experimental data showed a good prediction of the frequency and amplitude of the oscillations. Stability analysis performed by Brennen [66] showed that chugging is usually sustained in the natural, manometer type, oscillation of the system.

CFD modelling of the chugging regime during the PPOOLEX experiments was carried out by Pättikangas et al. [67] using ANSYS Fluent. The Euler-Euler model was used model direct contact condensation. The heat transfer between steam and water was modelled using a Reynolds and Prandtl based Nusselt number correlation. Due to the high computational cost, the simulations were run in 2D-axisymmetric models. The results showed a qualitative agreement on the chugging oscillation and collapse. However, the Nusselt correlation was observed to under-estimate the condensation rate since it allowed small steam bubbles escape from the main chugging collapsing bubble. Tanskanen et al. [68] and Patel [69] used NEPTUNE_CFD and ANSYS Fluent respectively with the cell-based Hughes and Duffey correlation for the Nusselt number and obtained a better prediction for the heat transfer, which again showed quantitative good agreement with the PPOOLEX data in terms of bubble radius and frequency of collapse. Using the same Eulerian-Eulerian models, Pellegrini et al. [70] used a Rayleigh-Taylor instability model to simulate the direct contact condensation heat transfer during chugging.

Work done by KAERI [71, 72, 49] introduced the Steam Condensation Region Model (SCRM), based on previous work done by Gamble et al. [73]. The SCRM solves equations of mass, momentum, and energy in a control volume where steam condensed completely, and imposes single-phase liquid entrainment and condensate boundary conditions of the jet. Implementations of the SCRM were done in Star CCM+ and ANSYS Fluent showed good agreement to complete mixing transients. Applicability to thermal stratification and mixing transients was not provided.

EHS/EMS models were introduced by Li & Kudinov (2010) [4] to develop predictive capabilities for long-term thermal stratification and mixing transients induced by a steam injection through blowdown pipes. The models were implemented in GOTHIC, and successfully validated against the PPOOLEX STB and MIX experiments [52, 55, 56], which were performed with different steam mass fluxes, pool temperatures, blowdown pipe diameters, etc.

Lumped parameter correlations for modelling of PSP stratification were developed in [10] based on 3D analysis results with GOTHIC. However, no evidence of the GOTHIC validity for prediction of pool mixing were demonstrated.

4. EHS/EMS models

Modeling of direct contact condensation (DCC) is a challenge for contemporary codes. The small length and time scale of steam condensation phenomena requires very fine mesh and small time step when using CFD [10, 11, 12], making it unaffordable for long-term transients in a PSP. Lumped and 1D codes are inadequate for prediction of 3D, transient mixing phenomena. Moreover, containment codes such as GOTHIC [74], and other thermal hydraulic codes (e.g. RELAP5 [75]), do not have a model for prediction of the effect of steam blowdown into a pool. Available condensation models are mostly designed for pipe flow regimes such as bubbly, churn, film, etc.

To develop predictive capabilities for long-term thermal stratification and mixing transients, Li & Kudinov (2010) [4] introduced the concept of Effective Heat Source (EHS) and Effective Momentum Source (EMS) models. The main idea of the effective models is that, characteristic time and space scales of DCC phenomena are much smaller than characteristic time and space scales of development of thermal stratification and global circulation and mixing in the pool. It was postulate that individual details of small scale high frequency oscillations are lost due to the scale separation and only integral “net effects” of the DCC phenomena are important for mixing and stratification in a large pool. These effects are determined in terms of the heat (EHS) and momentum (EMS) sources induced by steam injection into the pool. The effective heat Q_{eff} and momentum M_{eff} sources can be computed using equations (1) and (2) respectively [5],

$$Q_{eff}(t) = \frac{1}{\Delta t} \int_{t-\Delta t}^{t} Q(\tau) d\tau \tag{1}$$

$$M_{eff}(t) = \frac{1}{\Delta t} \int_{t-\Delta t}^{t} M(\tau) d\tau \tag{2}$$

where the integrals represent the time-average of the instantaneous variations of the sources over a period Δt of time. These variations are due to the oscillatory nature of direct contact condensation. For example, the large scale motions of the liquid inside the pipe during the chugging regime, the small scale oscillatory bubble behavior, etc. The ultimate goal of the EHS/EMS models is to provide the effective heat and momentum sources through the chart shown in Figure 1. That is, they should be able to predict the condensation regime given the current steam and pool conditions, and derive its corresponding heat and momentum sources.

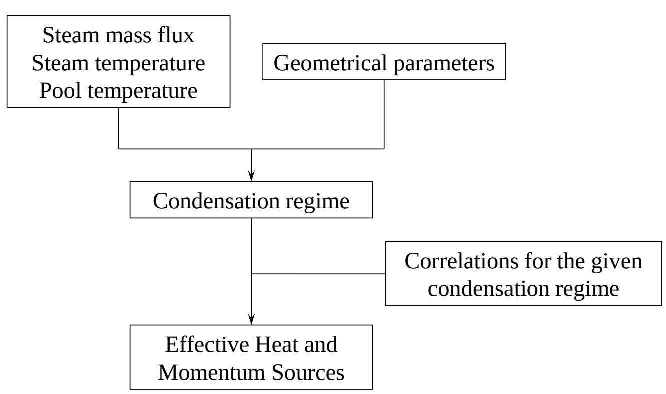

Figure 1: Calculation diagram of the EHS/EMS models

5. BLOWDOWN PIPES

EHS/EMS models for blowdown pipes were first developed and validated by Li et al. [5, 13] for the condensation regimes of chugging and complete condensation inside the pipe. Chugging is a condensation regime characterized by a periodic motion of the steam-liquid interface inside the blowdown pipe. This motion is driven by the pressure changes induced by the growth and collapse of large steam bubbles. In [5, 13], the effective momentum induced by chugging was obtained using an analogy to a "synthetic jet", a jet generated by an oscillatory flow through an orifice with zero time-averaged mass flow [76]. For a single harmonic oscillation, the velocity scale based on the momentum flux is given as equation (3),

$$U_{eff} = \sqrt{2} f A \tag{3}$$

where frequency f and A are frequency and amplitude of the oscillations respectively. Analysis of the PPOOLEX MIX data done in [5, 13] showed that, similar to a synthetic jet, the periodic motions of steam-water interface during chugging lead to the formation of a turbulent jet. In some cases, the momentum of the jet was sufficient to mix a thermally stratified layer. The effective velocity U_{eff} of the jet induced by the periodic motion was calculated using equations (4) and (5),

$$U_{eff} = \frac{2}{\pi}\overline{U} \tag{4}$$

$$\overline{U}(t) = \sqrt{\frac{1}{\Delta t}\int_{t-\Delta t}^{t} u^2(\tau)\, d\tau} \tag{5}$$

where u is the instantaneous velocity of the liquid level oscillations inside the blowdown pipe, $\overline{U}$ is velocity based on time-averaged square of the instantaneous velocity, and Δt is the averaging time scale of ~100 s. Equation (4) can be derived precisely for single harmonic oscillations. This approach was extensively validated against the PPOOLEX MIX 01-12 experiments [77]. Stratification, mixing, and re-stratification of a completely mixed pool were adequately predicted by the model.

The simulations performed in [13, 77] used the experimental data to calibrate the heat and momentum sources. However, as it was outlined in the Section 4, the EHS/EMS models should predict the condensation regime, and, based on this regime, predict the heat and momentum sources. Moreover, modelling of the feedback between pool temperature and drywell pressure was beyond the scope of the simulations done in [13, 77]. In this section, we present new correlations for the EHS/EMS models for blowdown pipes to predict the effective momentum induced by chugging, and the condensation regime (section 5.1), the implementation in GOTHIC for a coupled simulation of drywell and wetwell (section 5.2), and the validation against the PPOOLEX MIX-04 experiment (section 5.3).

5.1. EHS/EMS models for blowdown pipes

Work done by Villanueva et al. [29] showed that the frequency and amplitude of the liquid level oscillations in chugging (necessary to obtain the effective momentum, equation (3)) were well correlated with the Froude number, equation (6). Non-dimensional forms of the amplitude and frequency were also proposed in [29] as a function of the drywell volume V, pipe diameter d, submergence l_s, total pipe length l_p, and number of blowdown pipes n. The results showed good agreement with Aya & Nariai data [78].

$$Fr = \frac{G/\rho_s}{\sqrt{g l_s}} \tag{6}$$

It was mentioned in [29] that the use of the pipe length l_p as a scaling parameter should be further investigated. In this work, we decided to use the pipe submergence l_s instead of l_p, equation (8). The motivation is that the upstream parameter affecting chugging is the total gas volume V which accommodates a bubble collapse. Whether this volume is in the form of a pipe, drywell, or any other configuration, should have no effect on chugging.

The scaling factor used for the frequency in [29] was different than in the amplitude. However, since the frequency and amplitude of chugging oscillations should be correlated as $f \propto \sqrt{g/A}$ [79], its non-dimensional variables should also fulfil a relation of $\tilde{f}^2\tilde{A} \propto 1$. Thus, the frequency was scaled with the inverse square root of the scaling parameter of $\tilde{A}$, equation (9). Moreover, instead of using the pool temperature as in [29], the non-dimensional variables were plotted as a function of the pool subcooling, which is the driving potential for condensation. The effective velocity, equation (10) was also defined in terms of the previous non-dimensional variables. Table 1 shows the proposed non-dimensional variables, and Figure 2 its good agreement to the PPOOLEX MIX experiments (performed with 2 different blowdown pipe diameters) and to the Aya & Nariai data [78].

The data from Figure 2 was fitted to an Gaussian distribution using equation (7),

$$\tilde{\phi} = a e^{-\left(\frac{(\ln(Fr)-b)}{c}\right)^2} \tag{7}$$

where, a, b, and c coefficients reflect the influence of the pool temperature. Using the Non-Linear regression models from Matlab, individual a, b, and c coefficients were first obtained for 9 intervals of subcooling temperatures $T_s - T_p$ ranging from 120 to 80 °C, where T_s is the steam temperature inside the pipe and T_p the pool temperature. The resulting a, b, and c coefficients were then fitted to an analytical expression as a function of T_p and T_s ($\Delta T = T_s - T_p$). The final from of each coefficient is presented in Table 1, comparison to the experimental data in Figure 2, and its error in Figure 3.

Table 1: Scaling and coefficients of the analytical correlations for the amplitude and frequency of the chugging oscillations, and effective velocity of the turbulent jet.

	Non-dimensional variable	a	b	c	
Amplitude	$\tilde{A} = \frac{A}{l_s}\left(\frac{V/n}{l_s \pi d^2/4}\right)$	$\left(\frac{22.3}{0.16 + e^{-\Delta T/T_p}}\right)$	0.9	1.0	(8)
Frequency	$\tilde{f} = f / \sqrt{g \frac{V/n}{l_s l_s \pi d^2/4}}$	$\left(\frac{0.0019}{0.07 + e^{-(\Delta T/T_p)^{1.7}}}\right)$	$\left(\frac{0.21}{0.19 + e^{-(\Delta T/T_p)^{1.4}}}\right)$	1.0	(9)
Effective velocity	$\widetilde{U_{eff}} = U_{eff}\sqrt{\frac{V/n}{g l_s l_s \pi d^2/4}}$	$\left(\frac{0.17}{0.034 + e^{-(\Delta T/T_p)^{1.5}}}\right)$	$\left(\frac{0.29}{0.27 + e^{-(\Delta T/T_p)^{1.23}}}\right)$	0.7	(10)

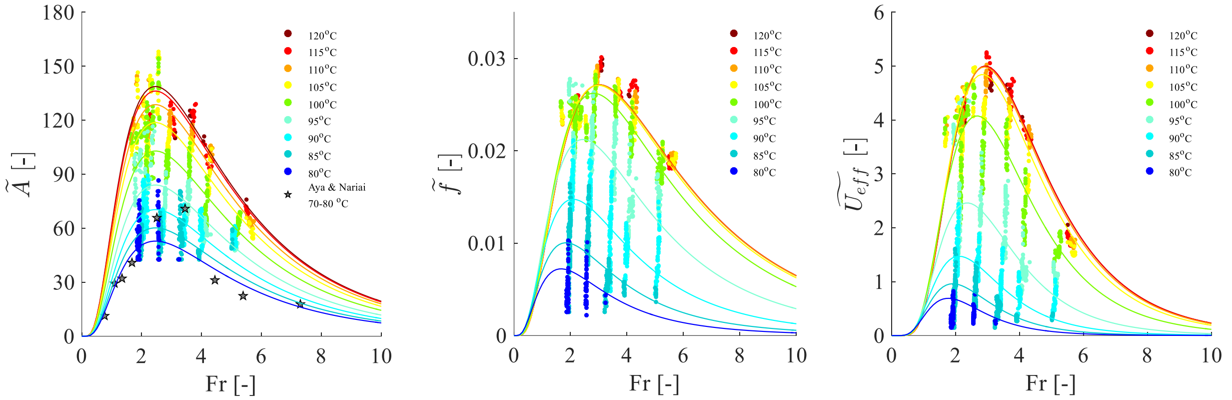

(a) (b) (c)

Figure 2: Scaling of the non-dimensional (a) amplitude, (b) frequency, and (c) effective velocity of the chugging oscillations. Symbols (○) corresponds to the MIX 01-12 experiments, (⋆) to Aya & Nariai data [78], and solid lines to the analytical correlations given in Table 1. The color band represents the subcooling ($\Delta T = T_s - T_p$).

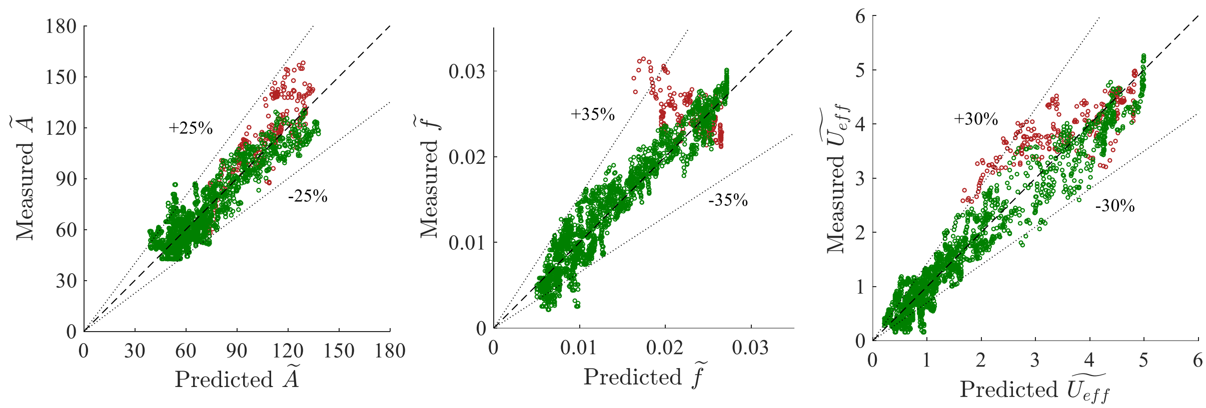

(a) (b) (c)

Figure 3: Fitting error of the non-dimensional (a) amplitude, (b) frequency, and (c) effective velocity of the chugging oscillations. Red and green dots correspond to the MIX 01-06 and MIX 07-12, carried out with 214 and 109 mm diameter blowdown pipes respectively.

The correlation for the EHS/EMS models require a condensation regime map which controls when they are activated in a simulation. Petrovic de With et al. [34] combined the regime maps from Aya & Nariai [31] and Chan & Lee [21], and Liang & Griffith [32] into a 3D regime map which took into account the injection hole diameter. It was assumed in [34] that the boundary between chugging and oscillatory condensation increases linearly with the pipe diameter. This conclusion was based on the fact that Chan & Lee obtained a larger chugging domain (using a 51 mm pipe) than that obtained in Aya & Nariai (with an 18 mm pipe). This assumption was observed to contradict the PPOOLEX MIX experiments, performed with 109 and 214 mm pipes, where chugging was suppressed much earlier than what was predicted in [34]. Moreover, Petrovic de With et al. assumed that Chan & Lee used an injection pipe with 51 mm inner diameter; however, they used a 51 mm nominal pipe with 39 mm inner diameter [80, 81].

The regime map proposed by Lahey & Moody [3] was also found to deviate substantially from the POOLEX data. Thus, the transition boundary between chugging and complete condensation inside the pipe was modelled based on the PPOOLEX MIX experimental data (Figure 4). At high pool temperatures, the boundary seems to follow a vertical given by equation (11). At low pool temperatures, the MIX-07 experiment suggest a temperature-dependent boundary which can be modelled using equation (12). Temperature dependency is expected in the transition boundary; however, more experimental data is necessary to further validate the correlations proposed in equations (11) and (12).

$$G = 3.5 \tag{11}$$

$$T_p = 28.5 - 3.0G \tag{12}$$

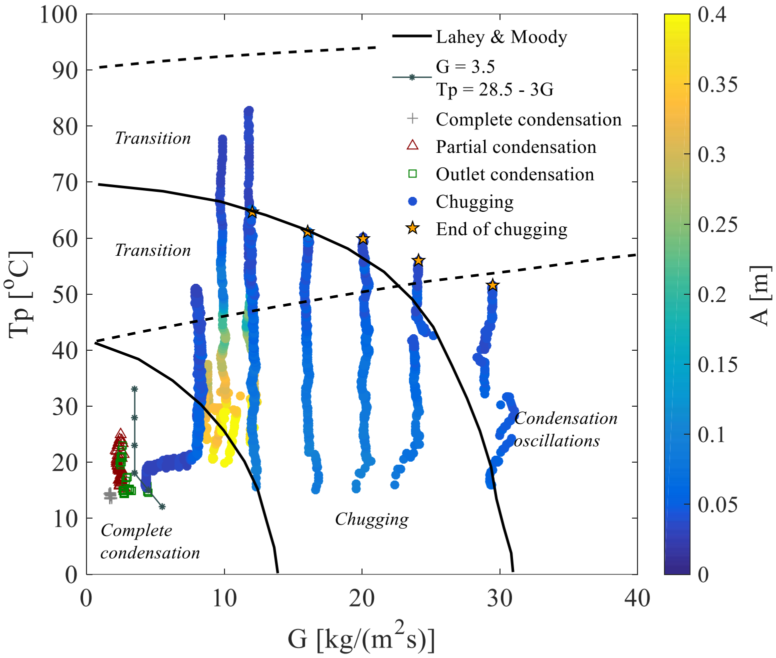

Figure 4: Steam condensation regimes during the PPOOLEX MIX experiments with blowdown pipe compared to Lahey & Moody regime map [3]. The Thermocouples (TC) inside the blowdown pipe were used to identify the condensation regime: (+) at least one TC measures the pool liquid temperature; (△) at least one TC measures a temperature between the liquid and the steam; (□) all the TCs inside the blowdown pipe measure steam temperature; (○) large scale oscillations between steam and liquid temperature, colored as a function of the amplitude of the liquid level oscillations inside the pipe; and (⋆) onset of small scale temperature oscillations in the pipe.

5.2. Implementation of EHS/EMS models in GOTHIC

In this section, we present the implementation of the EHS/EMS models for blowdown pipes in GOTHIC, for the integrated simulation of the wetwell and drywell during a prototypic LOCA transient in a BWR.

To use the EHS/EMS models presented in section 5.1, we need to monitor the pool and steam injection temperatures, and the steam mass flux through the blowdown pipes. This can be done by using control variables on the direct steam injection model presented in Figure 5a. However, allowing the blowdown pipe to inject steam directly into the wetwell prevents us from controlling the heat and momentum sources given by the EHS/EMS models. Moreover, this configuration may lead to numerical oscillations of the flow that can cause artificial mixing of the pool [4]. To overcome this issue, we propose the implementation of the EHS/EMS model presented in Figure 5b. Here, the flow path at the blowdown pipe outlet was connected to a pressure boundary condition ‘**2P**’ instead of the wetwell. Control variables were then used to set the pressure and temperature of this boundary condition, equal to the pressure and temperature of the pool at the blowdown pipe outlet. This allows simulating the wetwell and drywell behavior in an integrated manner, capturing the feedback between pool conditions and containment pressure.

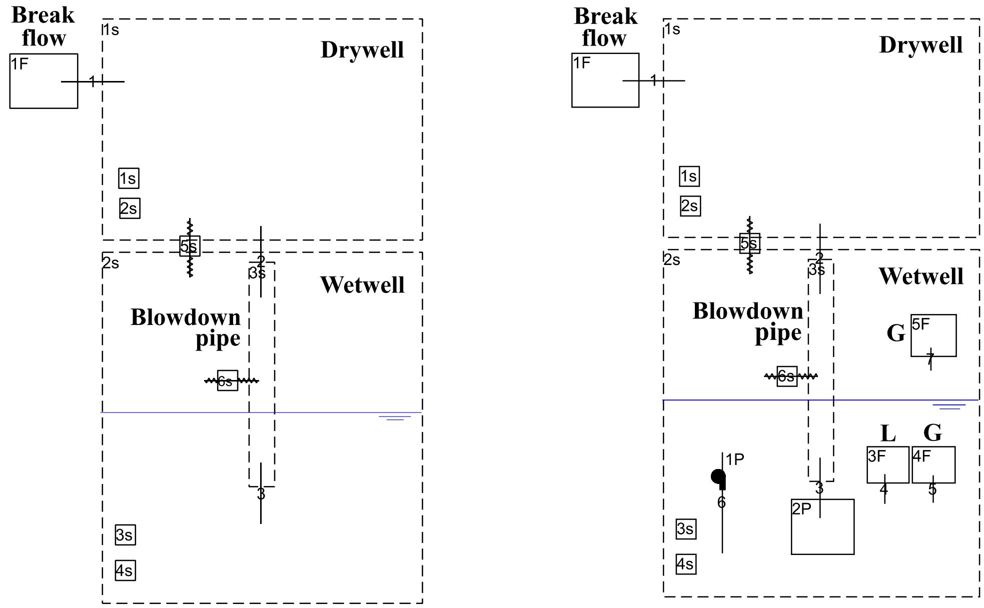

(a) (b)

Figure 5: GOTHIC models of a simplified containment using the (a) direct steam injection approach and (b) EHS/EMS containment model proposed in this work.

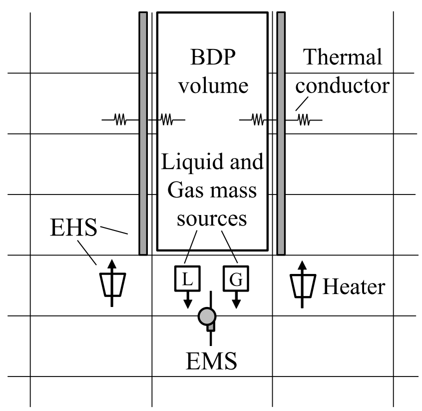

Figure 6: Detailed location of the boundary conditions in the EHS/EMS containment model.

To preserve mass in the EHS/EMS containment model proposed in Figure 5b, the water and gas flow rates injected into the pressure boundary condition were injected into the pool through flow boundary conditions '**3F**' and '**4-5F**' respectively (Figure 6). Since we do not intent to resolve direct contact condensation, un-condensed steam at the blowdown pipe outlet was injected in liquid phase. Flow rates with gas volume fractions lower than 0.01 were injected into the wetwell gas space through boundary '**5F**'. This was done to avoid the artificial mixing induced by a numerical stabilizer used by GOTHIC, which artificially increases the interfacial gas-liquid shear at low gas volume fractions. A thermal conductor was used between the blowdown pipe and the pool to allow predicting non-homogeneous heat flux profiles along the walls. The latent heat from the condensed steam was applied at the blowdown pipe outlet using heat sources.

The effective momentum was applied using a pump, which represents a source in the momentum equation. For the chugging regime, the activation of the pump was controlled with equations (11) and (12) and its effective injection velocity with equation (10).

In GOTHIC, simulating direct contact condensation of steam into water leads to numerical oscillations of the flow which can cause artificial mixing of the pool. This observation is not specific to the cases analyzed in this work, but to all previous simulations performed with different meshes, numerical, and geometrical parameters [4, 82, 83]. The GOTHIC models presented in Figure 2 are both prone to develop these oscillations due to the condensation of steam inside the blowdown pipe. However, the effect can be minimized when using the EHS/EMS containment model by time-averaging the oscillations at flow path '**3**' before injecting the flow through boundary conditions '**3-5F**'.

The model used to time-average the oscillations was an exponentially weighted moving average; that is, a Low-Pass (LP) filter. However, since LP filters cannot preserve the integral of a quantity after a step function, we developed a so called modified Double Exponential Smoothing (DES). Here, the LP filter of the High-Pass (HP) filter is added to the first LP filter, equations (13)-(16). We can see in Figure 7 that the modified DES produces a more stable and solution that converges faster to the original function than the previous DES models proposed in the literature. Therefore, the modified DES method was used to time-average the flow oscillations in GOTHIC.

$$\mathrm{LP}(x^i) \qquad y_1^i = \alpha x^i + (1-\alpha) y_1^{i-1} \tag{13}$$

$$\mathrm{HP}(x^i) \qquad y_2^i = (1-\alpha)\left(x^i - y_1^{i-1}\right) \tag{14}$$

$$\mathrm{LP}(\mathrm{HP}(x^i)) \qquad y_3^i = \alpha y_2^i + (1-\alpha) y_3^{i-1} \tag{15}$$

$$y^i = y_1^i + y_3^i \tag{16}$$

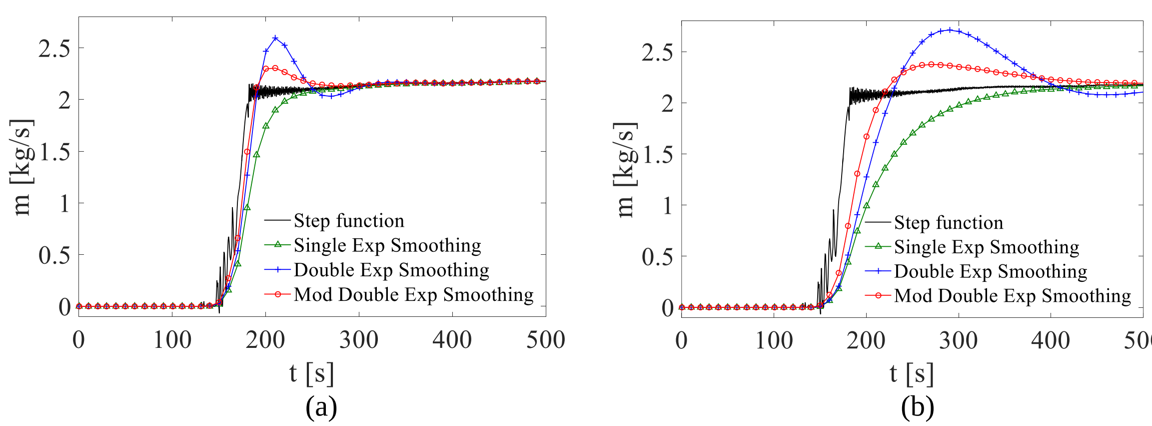

Figure 7: Single, double, and modified double exponential smoothing of a step function using a cutoff frequency of (a) 0.01 Hz and (b) 0.003 Hz.

5.3. Validation against PPOOLEX MIX-04 experiment

In this section, w present the validation of the EHS/EMS models for blowdown pipes presented in Sections 5.1 and 5.2 against the PPOOLEX MIX-04 experiment [55]. In this experiment, the wetwell was initially filled with a 2.13 m pool, and a 214 mm diameter blowdown pipe was submerged 1.7 m into the pool and connected to the drywell floor. The gas spaces of the drywell and wetwell were initially filled with air. Similar to a LOCA scenario in a BWR, steam was injected into the drywell. The experiment consisted on an initial clearing phase where a high steam injection pushed all the non-condensable gases into the wetwell gas space; a stratification phase at lower steam flow rates, and a mixing phase where the steam flow was increased to induce chugging.

The control volumes used in this model were the same as the ones presented in Figure 5b. A 3D mesh was used in the drywell and wetwell to capture the gas clearing and the thermal stratification phases respectively. A mesh sensitivity study was performed, and, similar to the results from [13], it was observed that a 50 mm mesh is required in the vertical direction to resolve the sharp temperature gradients in the pool.

The pressure and flow boundary conditions from Figure 5b were controlled as described in Section 5.1. For the time-averaging of the numerical oscillations at the blowdown pipe outlet, a cutoff frequency of 0.003 Hz was selected for the water, and 0.02 Hz for the gas. The condensation regime was identified using equations (11) and (12), and the effective momentum induced by chugging was computed using effective velocity from equation (10). The gas flow injection was switched from the wetwell pool to the wetwell gas space when the gas volume fraction was lower than 0.01.Thermal conductor '**6s**' and the heater from Figure 6 were used by the EHS model to provide the latent heat from condensation.

The k-Epsilon turbulence model was used in all of the control volumes with a turbulent Schmidt and Prandtl numbers of 1. The simulation was run using the Bounded Second Order Upwind (BSOUP) in space, and Semi-Implicit in time. The residuals were set to 1.0e-8, and the time step was allowed to vary between 1.0e-7 and 0.02 s. To avoid instabilities at the pool surface, the Surface Wave Damping Factor was set to 3 and the liquid shutoff volume fraction to 0.005. A direct steam injection of the MIX-04 experiment was also run using the same control volumes as in Figure 5a. The mesh, steam injection conditions, initial conditions, and numerical parameters were the same as the ones described for the EHS/EMS containment model.

We can see Figure 8 that thee pool liquid level and average pool temperature were accurately reproduced in the simulations. The small deviations in the average pool temperature during the stratification phase are attributed to the fact that it was estimated based on a limited number of TC measurements. At the end of the transient, when the pool is completely mixed and all the TCs give approximately the same temperatures, we can see that the difference between experimental and predicted temperatures decreases.

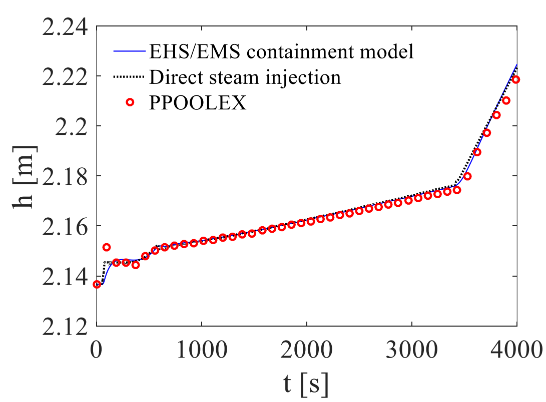

(a)

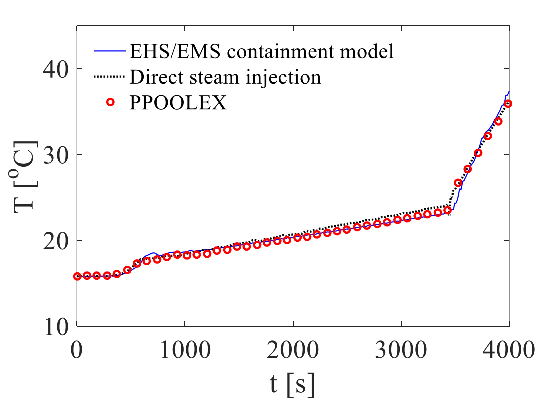

(b)

Figure 8: Comparison of the (a) liquid level and (b) average pool temperature obtained in GOTHIC and measured in the MIX-04 experiment. The average temperature was obtained as a spatially weighted average of all the thermocouples located in the pool.

During the stratifications phase the pool surface temperature measured in PPOOLEX was very well predicted when using the EHS/EMS containment model, Figure 9. This is due to the time-averaging model, which prevented the numerical oscillations at the blowdown pipe outlet from entering into the pool; and to the gas flow boundary condition in the wetwell gas space, which prevented small gas volume fractions to enter into the pool and induce artificial mixing. In the mixing phase, transition to chugging was observed and the EMS model provided the effective momentum given by equation (10). We can see in Figure 9 that the mixing trend was very well predicted, leading to a mixing time of 350 s, similar to the 400 s obtained in the PPOOLEX experiment. The Root Mean Square (RMS) error was computed for all TCs in the pool, and for the TC at the pool surface (2105 mm) using equation (17), where T_{PP} and T_G correspond to the PPOOLEX and GOTHIC temperatures respectively. The RMS of all simulations are given in Table 2.

$$RMS = \sqrt{\frac{\sum_{i=1}^{N}\left(T_{PP_i} - T_{G_i}\right)^2}{N}} \tag{17}$$

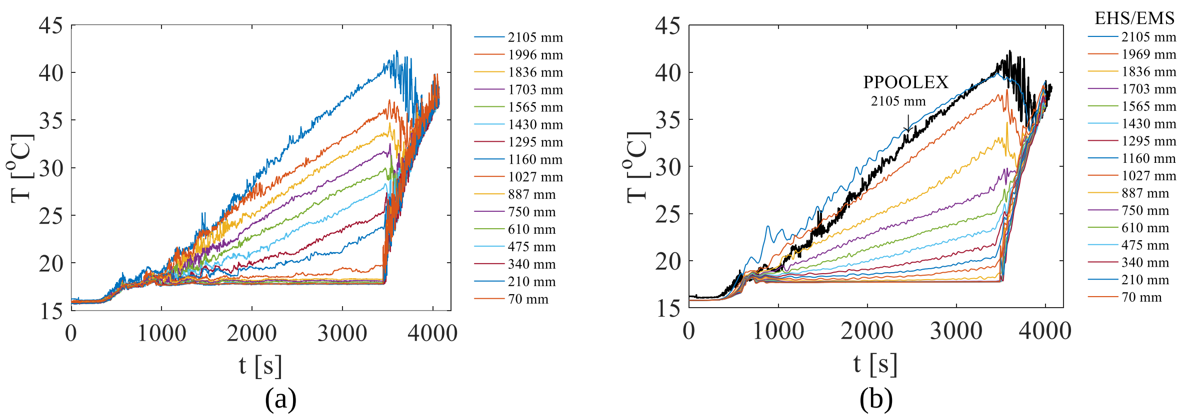

Figure 9: Pool temperature distribution obtained in with the (a) PPOOLEX MIX-04 experiment, and (b) EHS/EMS containment model.

Table 2: Root Mean Square (RMS) errors of the pool temperature obtained in the GOTHIC simulations with respect to the PPOOLEX-MIX 04 experimental data.

Simulation	Whole pool RMS [°C]	Pool surface z = 2105 mm RMS [°C]
EHS/EMS (Gas flow into WW pool or gas space)	0.36	1.71
EHS/EMS (All gas flow into WW pool)	0.46	2.20
Direct steam injection	0.77	3.70

The pressures predicted with the EHS/EMS containment model and the direct steam injection simulation were quite similar (Figure 10). This is due to a short stratification phase, in which differences in the pool surface temperature have a small effect on the pressure. However, it is expected that for longer transients, such as the one-day stratification in Fukushima Daiichi Unit 3 [9], the difference between the two models will be larger.

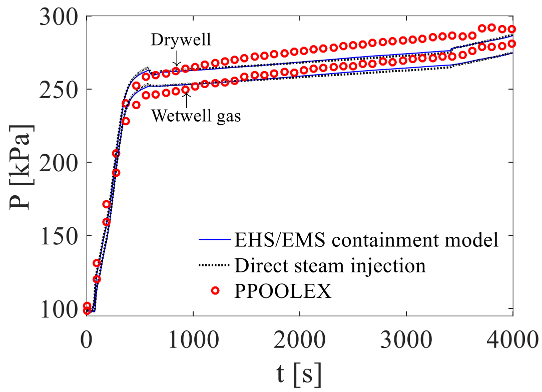

Figure 10: Pressure in the drywell and wetwell gas spaces obtained in the simulations and measured in the PPOOLEX MIX-04 experiment.

When using the direct steam injection approach, the numerical oscillations of the flow and the artificial high shear at high volume fractions led to partial mixing of the pool from (Figure 11a). By the end of the stratification phase the pool surface temperature was under predicted by about 9 °C (a value which would have continued to increase in a longer transient) with an overall RMS error of 3.7 °C (Table 2). Since GOTHIC does not have a model to predict chugging, the mixing phase could not be adequately predicted. The higher steam flow during this phase led to a strong buoyancy driven pattern which caused a much faster mixing of the pool than in the experiment. This result is an example of compensation of errors, where qualitatively correct results (mixed pool) are obtained for the wrong reasons (buoyancy driven flow).

Figure 11b presents a simulation run using the same EHS/EMS containment model as for Figure 9b, but injecting all the gas flow into the wetwell pool. We can see that, though having lower artificial mixing than in the direct steam injection simulation, gas flow as low as 0.2 g/s induced an artificial mixing which delayed the onset of stratification after the clearing phase.

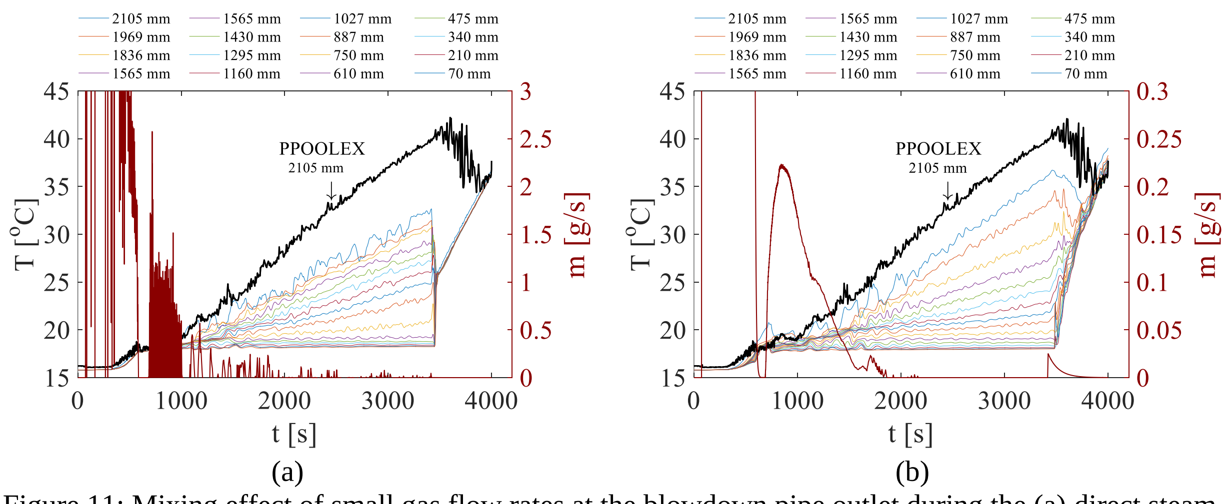

Figure 11: Mixing effect of small gas flow rates at the blowdown pipe outlet during the (a) direct steam injection simulation and (b) EHS/EMS containment model, injecting *all* the time-averaged gas flow into the wetwell pool. Second axis corresponds to the gas flow rate at the blowdown pipe outlet.

6. SPARGERS

Spargers are multi-hole injection pipes which discharge steam from the primary circuit into the PSP. They are also used in the exhaust of safety systems such as the RCIC [9]. The multi-hole injection leads to different condensation regimes than in the blowdown pipes, and thus, requires further development of the EHS/EMS models. Sections 6.1 and 6.2 present the scaling and analysis of the experimental data obtained in the PPPOLEX and PANDA experiments with spargers. Sections 6.3 and 6.4 the development and validation of the EHS/EMS models against the PANDA experiments.

6.1. Scaling of the PPOOLEX and PANDA experiments

The sparger experiments were scaled to preserve ranges of parameters and regimes that determine most important physical phenomena appearing in plant scale. Since all phenomena cannot be preserved simultaneously in a reduced scaled facility such as PPOOLEX or PANDA, the experimental data will not be extrapolated to plant. Instead, it will be used for analysis of the physical phenomena and code development, which, once validated, can be applied to predict plant behavior.

The scaling approach used in this work was based on the roadmap to scaling proposed by D'Auria & Galassi [84]. The plant selected for the scaling was a BWR Mark II, and the scenario a Station Black Out (SBO) where the ADS signal is received, causing 8 relief vales to open and discharge steam into the suppression pool through 4 spargers each [85]. In terms of plant safety, the phenomena of importance for this transient are the development of thermal stratification, which induces accelerated pressure increases in the containment; the erosion and mixing of the stratified layer, which determines the time needed to restore the complete cooling capability of the pool; and the direct contact condensation of steam into water. The sparger selected for scaling was the Westinghouse design for a BWR Mark II plants. This sparger injects steam downwards through an upper ring known as the Load Reduction Ring, and radially outwards at the sparger head. The PPOOLEX and PANDA test series were mainly focused on analyzing the separate effect of the sparger head alone.

Given the selected plant transient and sparger type, the design parameters were selected in order to reproduce the phenomena of interest. These parameters are divided into the macro, meso, and micro scales [84]. In the macro scale, full-length could not be preserved due to the geometrical restrictions of the facilities. However, the pool depth was kept as close as possible to full scale due to its importance for natural circulation transients. The order of magnitude of the time-scales of mass, momentum, and energy were preserved by setting an adequate total injection hole given the available steam mass flow rates [85]. In the meso-scale, the ratio of sparger submergence to pool depth was kept similar to the values found in the literature. The sparger pipe diameter was selected to preserve a similar steam mass flux as in prototypic BWR conditions. This ensures a similar condensation regime inside the pipe, and thus, a similar distribution of heat and momentum sources in the pool. In the micro-scale (steam jets), work done by Sonin [86] and Li et al. [87] emphasize that two-phase flow phenomena cannot be scaled. Thus, prototypic parameters of injection hole diameter, chamfer, pitch to diameters, and fluid properties were preserved as close as possible to full scale spargers. Due to the limitation in steam mass flow, the large number of holes found in a BWR sparger could not be reproduced, and was limited to 32 in PPOOLEX. Table 3 shows the final parameters used in the design of the PPOOLEX experiments. These designs enabled studding the pool and steam jets phenomena for the sub-sonic condensation regimes occurring between 0 and 300 kg/m^2s. These regimes are expected to dominate a long-term SBO transient. A regime map of all the experiments performed in presented in Figure 12.

Table 3: Dimensions of the PPOOLEX and PANDA sparger experiments compared to prototypical BWR

	BWR [a]	PPOOLEX
Pool volume	2000-3300 m^3	13 m^3
Pool depth	6-11 m	3 m
Pool diameter [b]	18-21 m	2.4 m
Submergence ratio	70 %	70 %
Sparger pipe diameter	150 mm	68 mm
Injection holes diameter	10-12 mm	8 mm
Total injection hole area	10100 mm^2	2010 mm^2
Horizontal pitch to diameter	3.6	3.3
Vertical pitch to diameter	4.5	4.5

The instrumentation used in the PPOOLEX and PANDA experiments was composed of flow meters, pressure transducers, ThermoCouples (TC) inside the pool and sparger, Particle Image Velocimetry (PIV) in front of the injection holes and in the thermocline, and video images of the steam condensation.

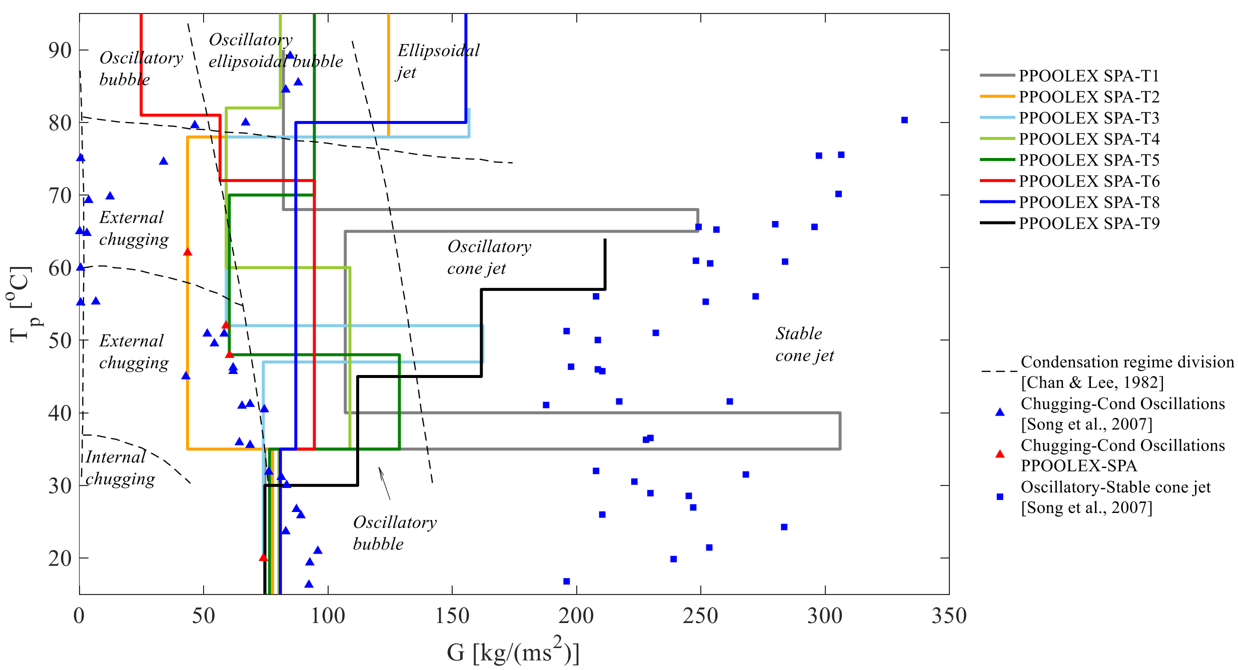

Figure 12: Condensation regime map of the PPOOLEX experiments with sparger, using Chan & Lee [21] and Song et al. [14] data. G is the steam mass flux at the injection holes, and T_p the pool bulk temperature. Shakedown test SPA-T0 not included in the map.

6.2. Analysis of the experimental data

All of the experiments performed in PPOOLEX began injecting steam at low momentum to create a stratified pool. After reaching a certain temperature difference between the top and bottom of the pool, the mass flow was increased to erode the stratified layer. During the low steam injection phase, the jets were quickly driven upwards by buoyancy. This led to the formation of a sharp thermocline, which maximum thickness can be assessed as about ~50 mm between the bottom cold layer and the upper hot part of the pool (Figure 13).

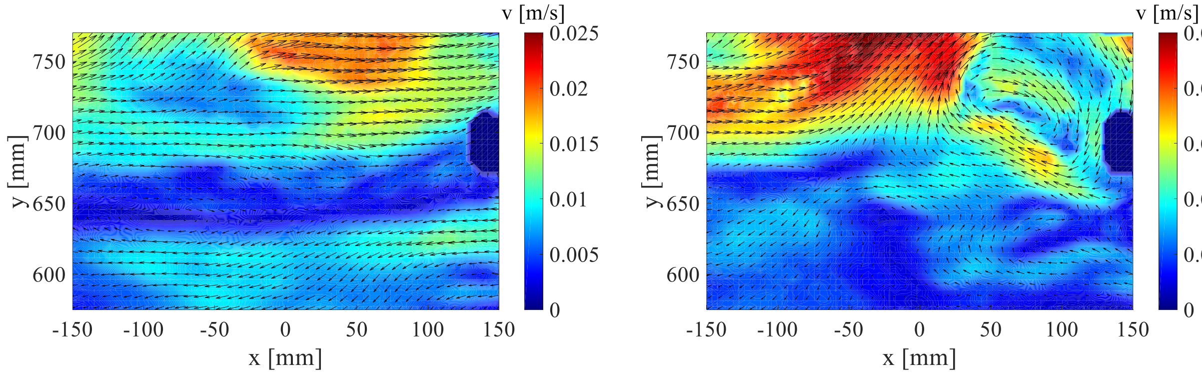

(a) (b)

Figure 13: Average velocity fields at the thermocline during the first stratification phase of the PPOOLEX SPA T8R experiment, (a) t = 3132.1 - 3135.7 s, contour plots generated using three dimensional velocity fields. Vector plots generated using x and y velocities. Every second vector displayed.

In the high steam injection phase, the jets inertia dominated, able to maintain their radial orientation until reaching the pool walls. During this phase, the TC measurements in the pool showed low frequency and large amplitude oscillations. A Fast Fourier Transform (FFT) analysis showed that these oscillations were similar to the first natural oscillation mode of the bottom layer (Figure 14).

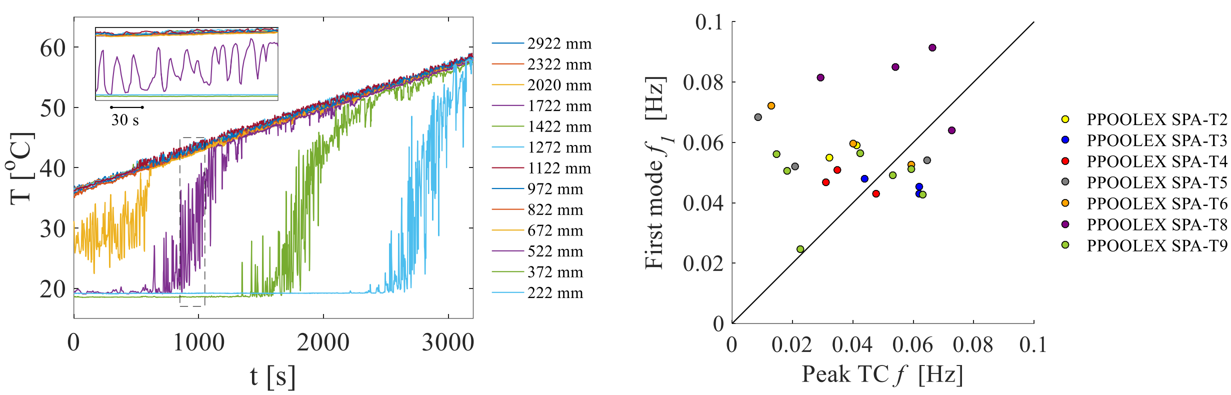

(a) (b)

Figure 14: Temperature oscillations at the stratified layer observed during the (a) PPOOLEX SPA-T4 experiment and (b) comparison between the peak frequencies obtained with a FFT analysis and the first natural oscillation mode of the stratified layer.

During the high steam injection phase, the erosion modes of the bottom stratified layer were observed to be well correlated with the Richardson number, equation (18) [59].

$$Ri = \frac{\Delta b \; D}{U^2} \tag{18}$$

In equation (7), Δb it the buoyancy jump across the thermocline, U the flow velocity above the thermocline, and D the distance between the sparger injection to the thermocline. At low Richardson numbers, high momentum flow was able to penetrated into the stratified layer, lift it, and mix it with the rest of the pool. This pattern could be observed by the all-at-once temperature increase in the TCs below the thermocline, and by the temperature drop in the TCs above it. We refer to this process as "mixing" of the pool. At higher Richardson numbers, the flow was only able to penetrate partially into the stratified layer, leading to the so called “erosion” regimes. This regime can be identified by the one-at-the-time temperature increase of the TCs below the thermocline (Figure 14a). Higher Richardson numbers prevented any flow from penetrating into the stratified layer. Turbulent eddies were only able to induce waves on the stratified layer, which would eventually grow and interact with each other, causing intermittent breakups and mixing events. This behavior can be observed in Figure 13b, where the PIV data shows an eddy destabilizing the smooth thermocline shown in Figure 13a. The waves induced by these eddies are expected to have a high frequency and small length scale, comparable to the size of the turbulent eddies. Thus, they do not correspond to large scale natural oscillation frequencies shown in Figure 14.

The vertical erosion velocity U_E of the stratified layer was estimated for all possible PPOOLEX experiments using the TC measurements in the pool. Similar to the conclusions from [59], the “erosion law”, equation (19), was observed to be applicable to the sparger induced erosion transients. Specific coefficients for the entrainment law were obtained through a non-linear fitting. The obtained correlation could be used in 1D models of a pool where, instead of resolving the weave breaking phenomena occurring at high Richardson numbers, the erosion velocity is directly estimated with equation (19), and imposed through, for example, a pump connecting the lower and upper parts of the pool.

$$\frac{U_E}{U} = C \cdot Ri^{-n} \tag{19}$$

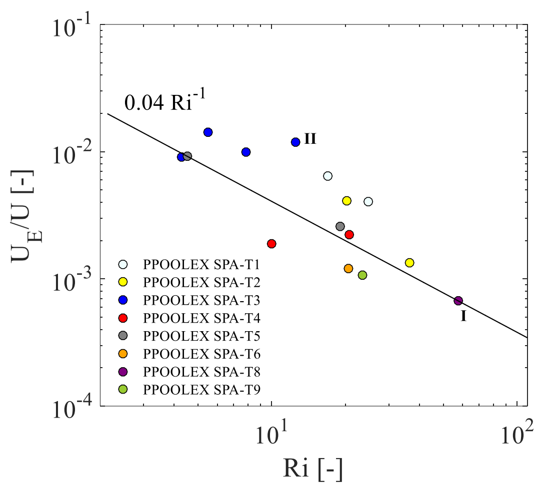

Figure 15: Richardson scaling of the velocity of erosion of a thermally stratified layer during the PPOOLEX experiments with spargers.

The condensation regime map from Figure 12 shows that most of the experiments were run in the oscillatory bubble regime. In this regime, bubbles grow, detach, and collapse from the injection hole at very high frequencies. Based on the injection hole diameter and subcooling, the frequency of this cycle for the PPOOLEX experiments can be estimated using Fukuda’s correlation [23] to be between 220 and 850 Hz. These frequencies were all above the acquisition rate of the instrumentation. Similar to stable jets, the oscillatory bubbles were observed to condense completely within ~50 mm (Figure 16a), which is about 6 injection hole diameters. After the condensation, the jets aligned in the same direction merged after a short distance (Figure 16b), similar to the distance of 3 times the pitch + diameter proposed by Ko et al. [88].

The TC data from PPOOLEX showed that the jets had a downwards orientation when released into the pool (Figure 16b). This was attributed to the downward velocity component of the steam inside the sparger. This velocity is not negligible since the area ratio between the sparger cross section and injection holes is about 0.5. Moreover, the sharp injection holes cannot re-direct the flow to a complete radial direction.

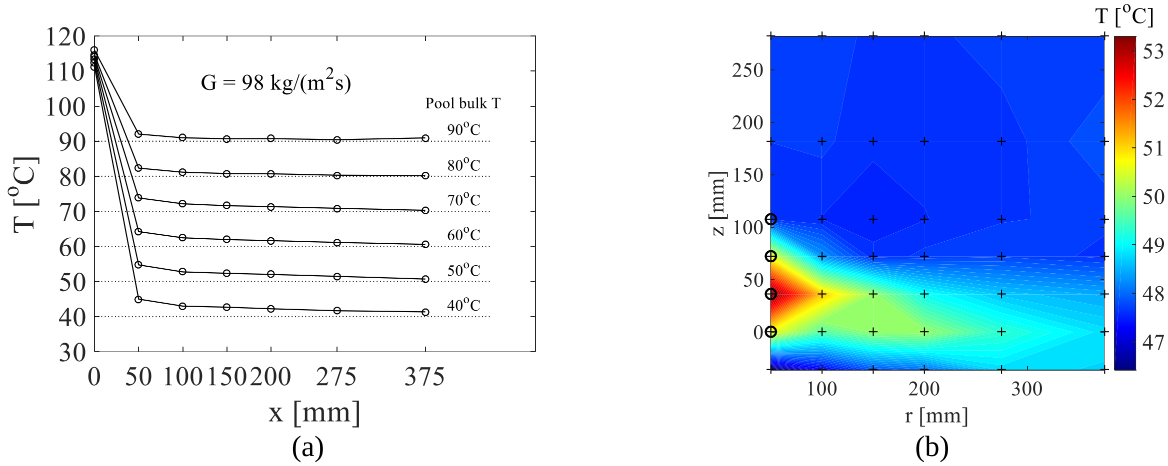

Figure 16: (a) PPOOLEX TC measurements in line with an injection hole as a function of the pool bulk temperature, and (b) temperature contours during the high steam injection phase of the PPOOLEX SPA-T3 experiment. TC data was time averaged over 200 s. Symbol (+) corresponds to the TC locations and (⊕) to first TCs in line with the injection holes.

The PPOOLEX SPA-T2 experiment (Figure 12) was an exploratory test to analyze the chugging regime. The low pool temperatures at the beginning of the test led to a strong chugging regime which caused a complete mixing of the pool. Re-stratification was observed when the pool temperature reached about 60 ^{o}C. This can be explained by the gradual decrease in the amplitude of the liquid level oscillations inside the pipe (Figure 17a), estimated based on the TC measurements inside the sparger. The frequency of the oscillations showed a much sharper decrease, which reached values close to zero at pool temperatures above 65 ^{o}C (Figure 17b). This led to a gradual reduction of the effective momentum, estimated using the same model as for blowdown pipes, equation (3), which allowed the re-stratification of the pool.

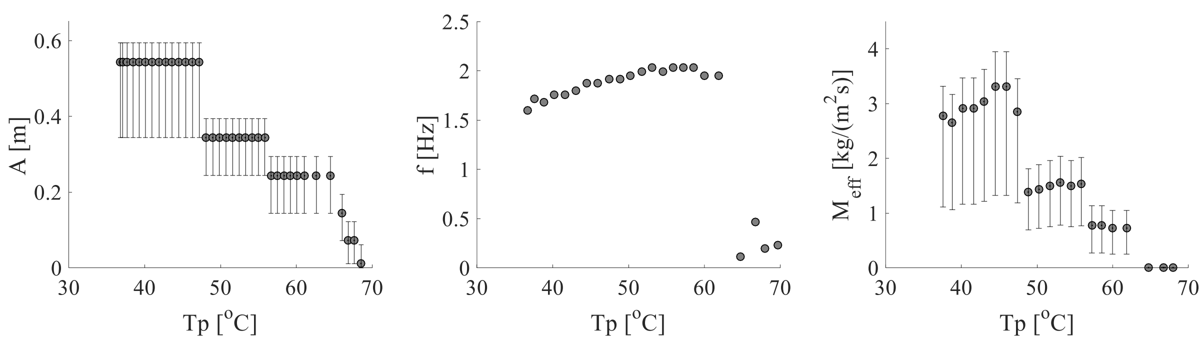

Figure 17: (a) Amplitude and (b) frequency of the liquid level oscillations inside the sparger as a function of the pool temperature, and (c) effective momentum induced into the pool. (No c

6.3. EHS/EMS models for spargers

When steam is injected into a subcooled pool, sonic flow develops at the outlet when the ambient pressure is lower than about 0.53 times the stagnation pressure P_0 upstream the nozzle. In these conditions, the pressure P at the nozzle outlet can be computed with equation (20),

$$\frac{P_0}{P} = \left(\frac{1+\gamma}{2}\right)^{\frac{\gamma}{1-\gamma}} \approx 0.53 \tag{20}$$

where γ is the heat capacity ratio of the injected fluid. If P is higher than the ambient pressure P_∞, the jet expands right after being released into the ambient [17]. This is known as an under-expanded jet. Since condensation is negligible during the expansion, the divergent shape of the steam cavity accelerates the steam to supersonic conditions, causing a second shock wave at the end of the expansion region. Successive expansion-contraction waves can be formed as the ambient pressure is further reduced. At a certain distance, sub-sonic flow is recovered, and the vapor contracts while condensing to generate an overall jet shape known as *ellipsoidal jet*. Outlet pressures P similar to P_∞ can reduce the length of the expansion region until no super-sonic effects are observed. This forces the jet to contract virtually from the beginning, giving the name of *conic jet*.

In conic and ellipsoidal jets, steam momentum is transferred to the liquid at the droplets entrained into the vapor core [89, 90]. Entrainment occurs through Kelvin-Helmholtz (KH) and Rayleigh-Taylor (RT) instabilities, triggered by the large shear forces at the steam-liquid interface. The liquid droplets are accelerated by the steam and become larger as steam condenses on their surface. After a certain distance, steam has condensed completely, and a single-phase liquid jet is created.

Using the control volume presented in Figure 18, a momentum balance in the axial direction for a sonic jet is given in equations (21). Here, Γ is the condensation flow rate, and sub-index i represents the fluid properties close to the interface. The steam and liquid momentum equations in the positive axial direction of the jet are presented in equations (22) and (23) respectively.

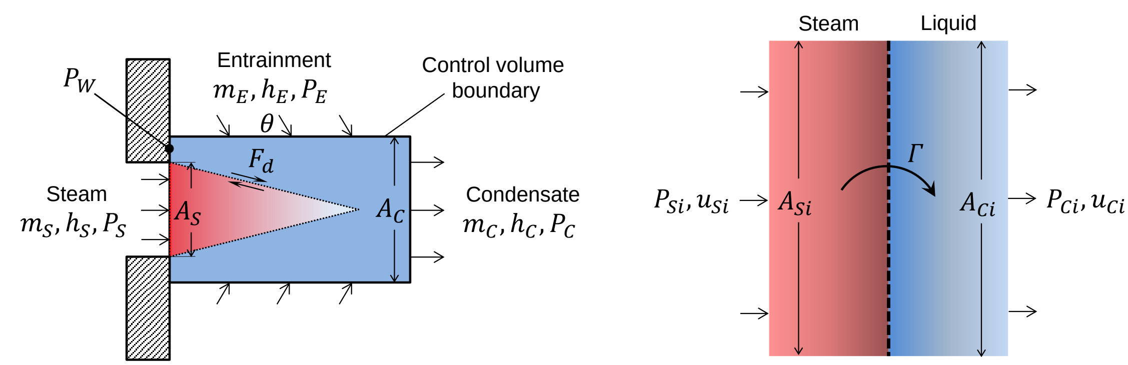

Figure 18: Steam condensation region.

$$\Gamma u_{Si} + P_{Si}A_{Si} = \Gamma u_{Ci} + P_{Ci}A_{Ci} \tag{21}$$

$$-m_S u_S + \Gamma u_{Si} = P_S A_S - P_{Si}A_{Si} - F_d \tag{22}$$

$$m_C u_C - m_E u_E \sin\theta \cos\theta - \Gamma u_{Ci} = -P_C A_C + P_w(A_C - A_S) + P_{Ci}A_{Ci} + F_d \tag{23}$$

In equations (22) and (23) the drag forces F_d should be equal for both phases but with opposite sign. We can also assume that the pressure near the sparger wall P_w is equal to the hydro static pressure of the pool at the injection holes level P_C. Moreover, since we expect the entrainment to be almost perpendicular to the direction of the jet, $\sin\theta$ will drop to a very low value and the magnitude of the entrainment term will be negligible. With these considerations, the summation of equation (21), (22) and (23) leads to equation (24).

$$\dot{m}_s u_s + P A_s = \dot{m}_c u_c + P_\infty A_s \quad (24)$$

From equation (24), the effective momentum M_{eff} is obtained as equation (25),

$$M_{eff} = \frac{1}{\Delta t}\int_{t-\Delta t}^{t} \dot{m}_c u_c(\tau)\, d\tau \approx \dot{m}_s u_s + (P - P_\infty) A_s \quad (25)$$

where the integral represents the time-averaged (effective) momentum over a Δt larger than the physical oscillations generated during the condensation [5, 13]. Since the flow rates and pressures in the cone and ellipsoidal jet regime are relatively stable, the integral can be further simplified to the injection and pool conditions.

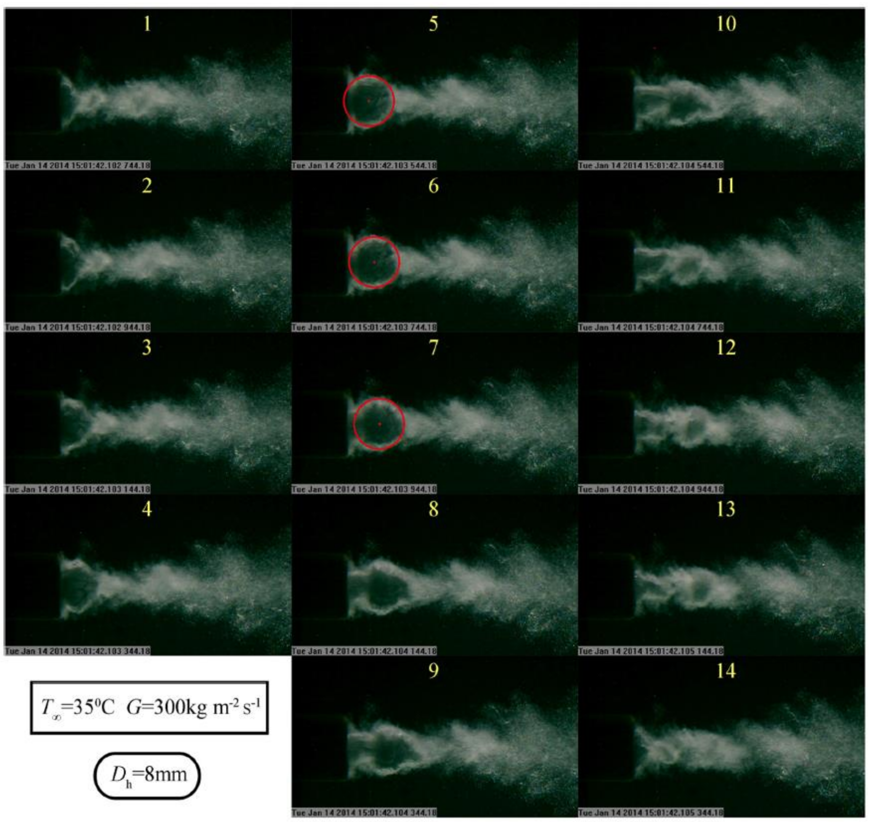

Figure 19: Oscillatory bubble regime. Image taken from [63]: *F. Yuan, D. Chong, Q. Zhao, W. Chen, J. Yan, Pressure oscillation of submerged steam condensation in condensation oscillation regime, International Journal of Heat and Mass Transfer 98 (2016) 193-203*.

When the steam mass flux is reduced below ~300 kg/(m^{2}s) the flow enters into the sub-sonic region. Here, the pressure at the outlet of the injection hole becomes equal to the ambient pressure ($P - P_\infty \approx 0$). The lower steam fluxes compared to sonic jets lead to a reduction in the KH and RT instabilities at the steam-liquid interface, decreasing the amount of liquid droplets entrained into the vapor core. This leads to the so called *oscillatory cone jet* regime, in which steam bubbles unable to condense within the vapor core are detached from the injection hole to condense trough a collapse [21, 22]. Further reductions of the steam mass reduce the entrainment of liquid droplets to a point where most of the condensation occurs at the detached bubbles. This corresponds to the *oscillatory bubble* regime, Figure 19. At very low steam mass fluxes the jet and bubble surface appear to be smooth, and condensation only occurs at the collapsing bubbles [26].

It is clear from the previous discussion that the oscillatory condensation regimes cannot be modelled with equation (25). This is because the momentum transfer of the collapsing bubbles is not considered. The effect of the condensation regime is modelled through the condensation regime coefficient shown in equation (26),

$$M_{eff} = C\dot{m}_s u_s \tag{26}$$

This coefficient is currently estimated based on the post-test CFD simulations of the PPOOLEX and PANDA experiments. Section 6.3.1 presents the experimental facility being built to get a direct measurement of C.

6.3.1. Separate effect facility

The goal of this facility is to measure directly the effective momentum induced by the oscillatory bubble regime. This would allow stablishing a map of the effective momentum as a function of the steam mass flux, pool subcooling, geometry of the injection hole, and number of injection holes. The experimental facility is currently under design by KTH and LUT. Construction of the facility is expected to occur during the summer, and experimental data should be obtained by the end of the year.

A preliminary design of the is presented in Figure 20. Similar to the sparger configuration, steam is injected into the pool in a horizontal direction. The sparger pipe is fixed at a point where it is able to rotate. The momentum of the steam at the injection hole can be measured at by the torque induced at the fixing point. The effective momentum (momentum transferred from the steam to the liquid) can be measured by placing a volume downstream the injection point. In this configuration, the torque measured at the fixing point is due to the momentum at the outlet of the added control volume (not the outlet of the injection hole). Entrainment into the added volume is enabled by opening a radial section around the injection point. Since the entrainment flow will be forced to flow in a radial direction, it will not affect the axial effective momentum.

Other measurements such as TCs, pressure transducers, and high speed cameras will also be used to get more details of the direct contact condensation phenomena. A sketch of the test procedure which will be used to map the effective momentum for a given injection hole geometry is presented in Figure 21.

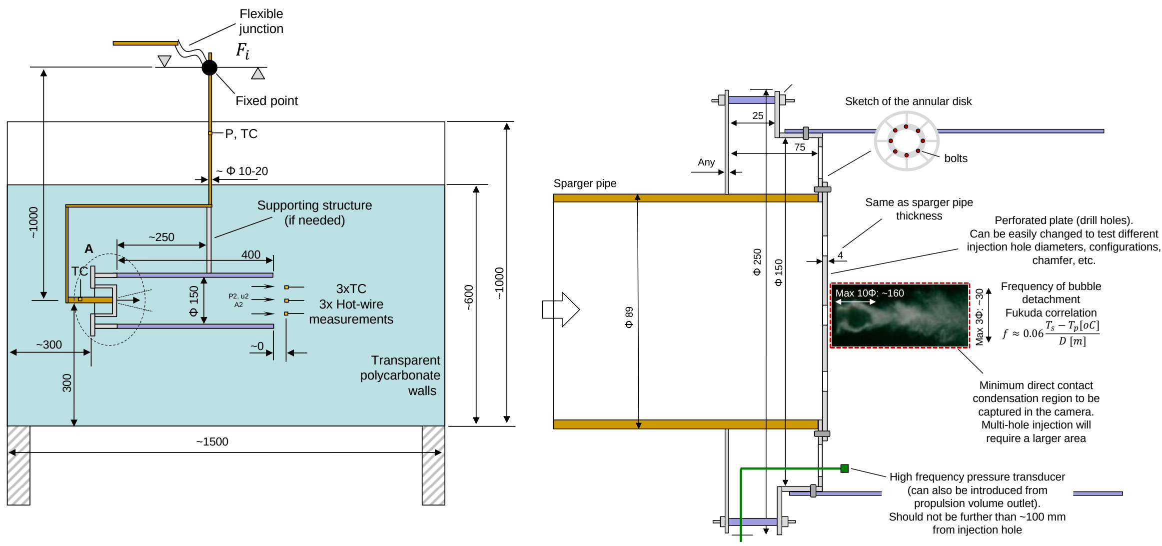

Figure 20: Preliminary design of the separate effect facility to be built in Lappeenranta University of Technology (LUT).

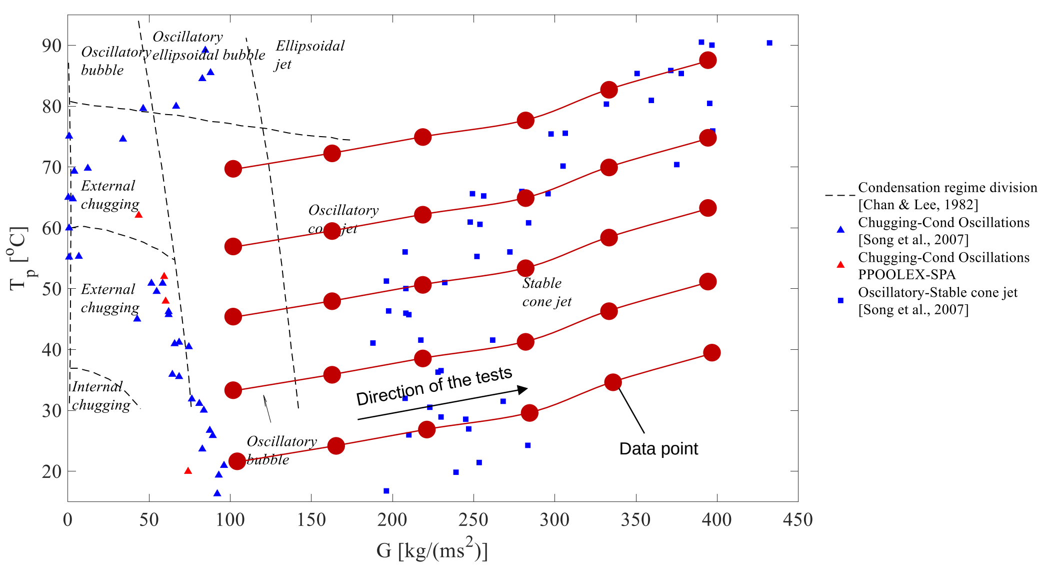

Figure 21: Test procedure to be followed during the experiments performed with the separate effect facility.

6.4. Implementation of the EHS/EMS models

The EHS/EMS models presented in Section 6.3 can be implemented in any computational platform. Initial implementations were done in GOTHIC due to its computational efficiency and containment analysis capabilities [91]. However, for the sparger, the radial steam injection could not be adequately captured using the Cartesian mesh from GOTHIC. Radial mesh should be used to minimize numerical diffusion of the jets transverse to the grid lines. For this case, Fluent becomes a more suitable choice. In this section, we present the most important modelling approached needed for the simulation of the pool transient in ANSYS Fluent 17.0.

6.4.1. Buoyancy effects on turbulence

As it was shown in Figure 13, low momentum injections through the sparger led to a stable thermally stratified layer, separated by a ~50 mm thick thermocline from the hotter layer above it. The sharp temperature gradients across the thermocline supress mean and turbulent vertical motions. This affects the stability of stratification, and the speed of erosion and mixing when the momentum is increased.

In a two-equation turbulence model, the buoyancy source term appears during the derivation of the turbulent kinetic energy k equation in the form of equation (27). This term is usually modelled using the Standard Gradient Diffusion Hypothesis (SGDH), equation (28), or by the Generalized Gradient Diffusion Hypothesis (GGDH), equation (29), which takes into account flow anisotropy. Though being more elaborate, the GGDH has been shown to be applicable mainly to flows governed by unstable stratification [94].

$$G = g_i \overline{u_i' \rho'} \tag{27}$$

$$G_{SGDH} = g_i \left(\beta \frac{\mu_T}{Pr_T} \frac{\partial T}{\partial x_i} \right) \tag{28}$$

$$G_{GGDH} = g_i \left(-\frac{\mu_T}{\rho Pr_T} \left(\frac{3}{2} \frac{\overline{u_i' u_j'}}{k} \right) \frac{\partial \rho}{\partial x_i} \right) = g_i \left(\beta \frac{\mu_T}{Pr_T} \left(\frac{3}{2} \frac{\overline{u_i' u_j'}}{k} \right) \frac{\partial T}{\partial x_j} \right) \tag{29}$$

Since the dissipation ε/ω equations are built in analogy to the k equation, buoyancy terms should also be present there. However, contrary to the turbulent production term due to shear P, the buoyancy term G can be positive or negative (acting as a producer or destroyer of k), questioning the need of a term in the ε/ω equations. To solve this issue, most CFD codes introduce a $C_{3\varepsilon}$ parameter which can be equal to 0, 1, or vary between 0 and 1. It implementation in the k, ε, or ω equations is presented in equations (30), (31), and (32) respectively.

$$\frac{Dk}{Dt} = P + G - \varepsilon + \Pi_k \tag{30}$$

$$\frac{D\varepsilon}{Dt} = C_{1\varepsilon} \frac{\varepsilon}{k} (P + C_{3\varepsilon} G) - C_{2\varepsilon} \frac{\varepsilon^2}{k} + \Pi_\varepsilon \tag{31}$$

$$\frac{D\omega}{Dt} = \alpha \frac{\omega}{k} (P + C_{3\varepsilon} G) - \beta \omega^2 + \Pi_\omega \tag{32}$$

Through Fluent default setting is $C_{3\varepsilon}$ = 0, it allows varying it between 0 and 1 depending on whether we are in stable or unstable stratification respectively. This is done through equation (33), which tends to zero when the vertical mean velocity V tends to zero. In [85], the authors decided to control $C_{3\varepsilon}$ using the well stablished correlation of the gradient Richardson number, equation (34). Theoretical [95, 96], and experimental [97, 98] works have shown that stable stratification occurs when Ri_g<0.2 and reaches complete instability at Ri_g>1. Based on this ranges, the $C_{3\varepsilon}$ can be controlled using equation (35).

$$C_{3\varepsilon} = \tanh(V/U) \tag{33}$$

$$Ri_g = \frac{\beta g \frac{\partial T}{\partial z}}{\left(\frac{\partial U_r}{\partial z}\right)^2 + \left(\frac{\partial U_z}{\partial z}\right)^2} \tag{34}$$

$$C_{3\varepsilon} = \begin{cases} 0 & Ri_g > 1 \\ -1.25Ri_g + 1.25 & 0.2 < Ri_g < 1 \\ 1 & Ri_g < 0.2 \end{cases} \tag{35}$$

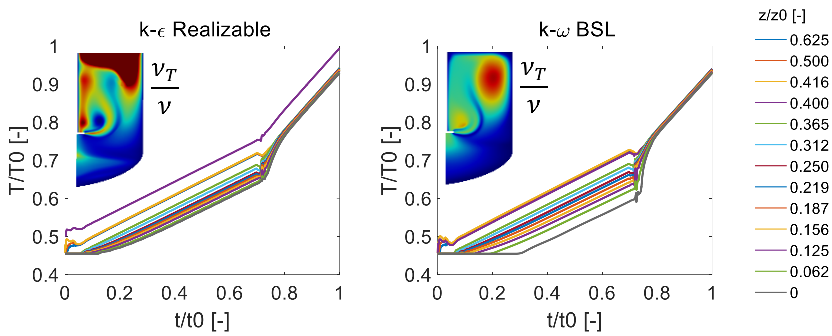

(a) (b)

Figure 22: Behavior of the (a) $k\varepsilon$-Realizable model using full buoyancy terms, (b) $k\omega$-BSL without any buoyancy effects.

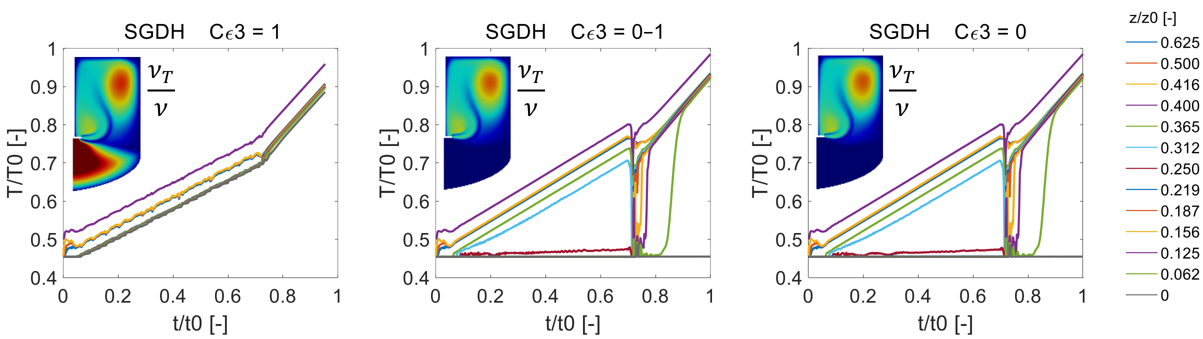

(a) (b) (c)

Figure 23: Be behavior of the $k\omega$-BSL model using the SGDH with (a) $C_{3\varepsilon}$=1, (b) $C_{3\varepsilon}$=[0-1], (c) $C_{3\varepsilon}$=0.

An extensive sensitivity study done by the authors in [85] showed that the behavior of the thermocline observed in the experiment was best predicted in Fluent when using the $k\omega$-BSL model with the SGDH and a $C_{3\varepsilon}$ varying between 0 and 1 (Figure 23). Though turbulent source terms due to buoyancy are not available in Fluent $k\omega$ models, they were added through UDFs. Using a $C_{3\varepsilon}$ equal to 1 led to a complete diffusion of the bottom stratified layer. In the $k\varepsilon$ model, Fluent allows using the built-in SGDH with a $C_{3\varepsilon}$ varying between 0 and 1. However, despite having taking buoyancy into account, the $k\varepsilon$ simulation resulted in complete diffusion of the stratified layer (Figure 22).

Another possibility to model buoyancy effects on turbulence is to damp the turbulent viscosity when the gradient Richardson number goes below the critical range of 0.2-1. However, damping the turbulent viscosity is a way to compensate for the incorrect modelling of the turbulent source terms due to buoyancy. This should be avoided for a robust application of a predictive model. Therefore, we preferred to include the source terms as described above.

6.5. Preliminary validation against PANDA HP5 experiments

In this section, we present the validation of the EHS/EMS models for sparger presented in Sections 6.3 and 6.4 against the PANDA HP5-1, and 2 experiments [85, 92]. Both of these tests began injecting steam at low steam mass flux, and increased after a certain temperature difference was achieved between the top and bottom of the pool.

The Volume Of Fluid (VOF) model was used in the whole domain to capture the rising liquid level of the pool. The k-Omega Baseline (BSL) model was used together with a UDF providing the turbulent source terms due to buoyancy using the SGDH and a $C_{3\varepsilon}$ varying between 0 and 1, equations (28) and (35). The Coupled solver (including volume fraction coupling) was observed to be more stable and to allow time steps one order of magnitude higher than Segregated solvers such as PISO. In the numerical schemes, the third order QUICK scheme was used in space and the bounded second order implicit in time. The residuals were set to 1e-5 for all of the variables except the energy, which was set to 1e-6. The effective momentum was obtained using equation (26) and assuming a condensation regime coefficient C = 1. Since the simulations were run using a 2D-axisymmetric model, it was implicitly assumed that the momentum source is uniformly distributed along the azimuthal direction. The momentum source was applied a radial distance of 250 mm far from the injection holes, a distance which is long enough to ensure that all of the steam jets have condensed completely.

The results show that the assumption of C = 1 led to a good prediction of the pool temperature profiles during the low and high steam injection phases (Figure 24 and Figure 25). We can see that during the low steam injection phase the location of the thermocline was predicted to be above that observed during the experiments. This deviation can be attributed to the downward inclination of the jets at the exit of the sparger injection holes observed in the experiment. Such inclination was not included in the model. The temperature in front of the injection holes, z/z0 = 0.4, was in a very good agreement to the experimental data. In the high steam injection phases, the erosion velocity was very well predicted in the HP5-1 experiment, but slightly over predicted in the HP5-2. The reasons for this deviation could be due to an over-estimation of the effective momentum, or to the assumption of uniform velocity profile of the jets.

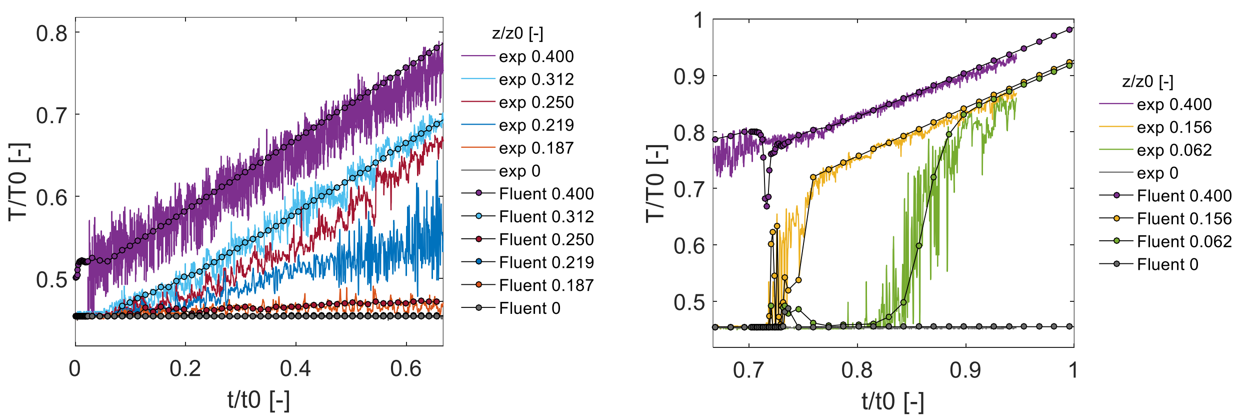

(a) (b)

Figure 24: PANDA HP5-1 simulation results using the k-Omega BSL turbulence model and the SGDH with $C_{3\varepsilon}$ = 0-1 and comparison to experimental data during the (a) low and (b) high steam injection phases.

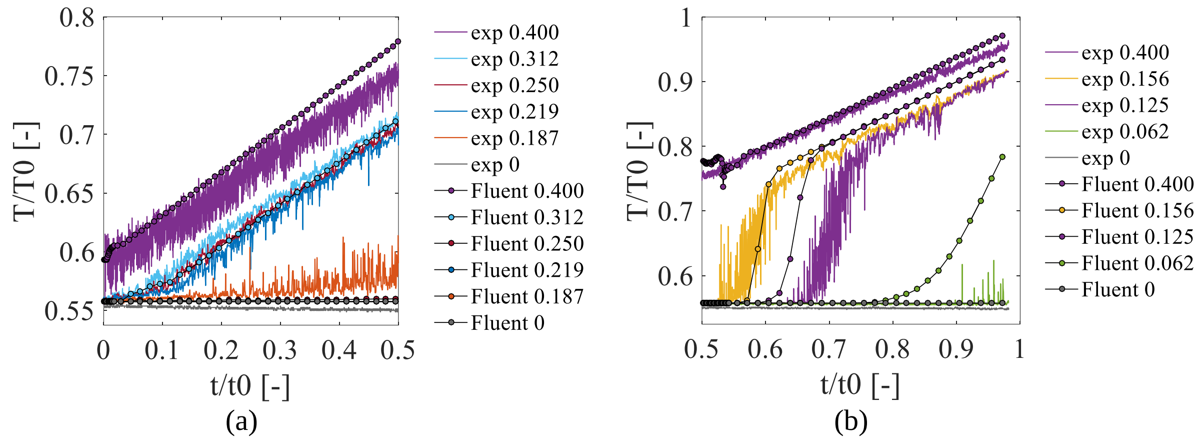

Figure 25: Simulation results of the PANDA HP5_2 experiment using the k-Omega BSL turbulence model and the SGDH with $C_{3\varepsilon}$ = 0-1 and comparison to experimental data during the (a) low and (b) high steam injection phases.

7. MIXING NOZZLES

In a BWR, mixing nozzles inject water at high momentum into the wetwell pool to break any thermal stratification that might develop. Usage of this system could occur, for example, in a SBO where power supply is suddenly recovered. In this section, we present the scaling, pre-test, and experimental campaign done with mixing nozzles in the PPOOLEX facility to investigate the effect of different injection parameters in the mixing efficiency.

The mixing nozzles are part of the Residual Heat Removal (RHR) system, which drains water from the wetwell pool and returns it cooled to the wetwell through strainers and nozzles. In a prototypic Nordic BWR, the strainers are long perforated plates or cylinders with a total injection hole are of about 1 m^2 per train. With such large area, the momentum of the water injected through them is small and they are not expected to be able to mix the pool. Since nozzles inject large amount of water through much smaller orifices, the momentum is much larger than in the strainers, and thus, they will be the dominant mixing mechanism during the RHR functioning. Prototypical nozzle designs in Nordic BWRs are presented in Table 4. We can see that there are several nozzles in the wetwell. However, only one of them injects a substantial amount of momentum which can induce mixing. For this reason, the PPOOLEX experiments with mixing nozzle were scaled to induce a similar behavior as Nozzle 2.

Table 4**: Liquid injection conditions of the mixing nozzles in a prototypic Nordic BWR.**

Mixing nozzles in a BWR	Liquid flow rate	Diameter of the nozzle	Reynolds number at exit [a]	Momentum of the injected liquid [a]
Nozzle 1 (×2)	10 kg/s	0.033 m	4.8e5	117 kg·m/s^2
Nozzle 2 (×1)	170 kg/s	0.12 m	2.2e6	2542 kg·m/s^2

[a] Assuming liquid injection at 30 ^oC: μ = 8e-4 kg/(ms), ρ = 1000 kg/m^3

7.1. Scaling of the PPOOLEX and PANDA nozzle experiments

Similar to the scaling of the sparger presented in Section 6.1, the goal of the scaling was to preserve prototypical ranges of injection conditions and pool regimes occurring during a liquid injection through the mixing nozzle from Table 4. Since the spatial and temporal scales of all the processes occurring at full scale cannot be preserved simultaneously in a reduced-scale facility such as PPOOLEX, we will emphasize that it will not be possible to extrapolate the experimental results obtained with the scaled design to predict what would happen in full scale. The experimental results will be mainly used for code validation.

In our scaling methodology, the design parameters were divided into similar groups as in the sparger: macro-scale (water pool) and micro-scale (injection holes). Details of each section are given below.

In the macro-scale, the pool depth was set equal than in the sparger experiments; that is, 3 and 4 m for PPOOLEX and PANDA respectively. The ratio of submergence of the nozzle to pool depth was kept similar to the 16 % value found in Nordic BWRs. In PPOOLEX, the nozzle was located at the center of the pool, allowing vertical and horizontal injection. In PANDA, it was located close to the wall oriented horizontally and with an angle to create a swirling motion in the pool, similar to the arrangement found in Nordic BWRs.

Macro-scale (water pool): The goal is to study different regimes of pool mixing by the momentum injected through the nozzle. To induce a similar thermal behavior in the pools, we should preserve ranges of mass, momentum, and energy time scales, and spatial similarity between the PPOOLEX and BWR pools. To achieve this goal, the design parameters needed to be determined are the (i) pool depth, (ii) location of the nozzle, (iii) orientation of the nozzle, (iv) liquid mass flow through the nozzle, and (v) total injection hole area. The selection of the design parameters is given below.

(i) The pool depth was set to 3 m, the same value as the one used in the sparger experiments. This depth gave a good spatial similarity between the water volume around a *single* sparger in a BWR, and the PPOOLEX pool. However, since there is only *one* mixing nozzle in a BWR (Nozzle 2 in Table 4), its area of influence is the whole pool. The prototypic height to diameter ratio of a BWR pool is about 0.3; whereas in PPOOLEX, with the chosen 3 m pool depth, it is 1.25. Therefore, the pool behavior induced by the nozzle in PPOOLEX is expected to be more affected by confinement effects, such as interaction with the walls, than in the BWR pool.

(ii) The nozzle was located in the center of the pool and submerged 0.5 m below the surface. Prototypical submergences of the mixing nozzles in a BWR are about 15 % of the wetwell pool depth. In our case, the 0.5 m submergence in the 3 m pool leads to a similar ratio of 16 %. In a BWR, the nozzles are usually located close to the wall since the RHR piping is arranged around the wetwell walls. However, we decided to locate the nozzle in the center of the pool to allow a more efficient validation of the models.

(iii) The nozzle was designed to allow both horizontal and vertical downwards injections. In a BWR, Nozzle 2 is near the wall, oriented horizontally and with an azimuthal angle of about 45^o which would induce a rotating flow pattern in the pool. Due to the already high spatial distortions between the PPOOLEX and BWR pools, we decided to maintain the nozzle in the center of the pool, injecting horizontally and vertically, without inducing the rotating flow pattern in the pool. The vertical injection, despite not found in the BWRs, would allow a more efficient validation using 2D axisymmetric models.

(iv, v) Given the aforementioned pool dimensions, the order of magnitude of the mass, momentum, and energy time scales were preserved by setting a total injection hole area of 64 mm^2 and a liquid mass flow of 1 kg/s. The mass time scale, equation (36), was defined as the ratio of mass injected into the pool to mass in the pool. The momentum time scale, equation (38), was defined as the momentum rate injected through the nozzle to the potential energy needed to mix the pool. The energy time scale, equation (37), was defined as the ratio of energy rate injected into the pool to the energy of the pool.

$$\omega_m = \frac{\dot{m}_{nzl}}{m_L} \tag{36}$$

$$\omega_p = \frac{\dot{m}_{nzl} v_{nzl}}{m_L \sqrt{gH}} \tag{37}$$

$$\omega_e = \frac{\dot{m}_{nzl} h_{nzl}}{m_L h_L} \tag{38}$$

In the equations, m, $\dot{m}$, h, and v are the mass, mass flow rate, enthalpy, and velocity of the fluid; sub-indexes nzl and L the nozzle and pool respectively. H is the total height of the pool and g the acceleration due to gravity. The results are presented in Table 5. We can see that the time scales are in the same order of magnitude, suggesting that similar thermal behavior of the BWR and PPOOLEX pools can be expected. However, this is something which will need to be verified in section 7.2 with the pre-test simulations since it is also influenced by the confinement of the PPOOLEX vessel and the flow field.

Table 5: Energy and momentum time scales during a liquid injection through the mixing nozzles

	Mass time scale ω_m [1/s]	Momentum time scale ω_p [1/s]	Energy time scale ω_e [1/s]
BWR[a]	$8.5 \cdot 10^{-5}$	$1.7 \cdot 10^{-4}$	$8.5 \cdot 10^{-5}$
PPOOLEX	$7.9 \cdot 10^{-5}$	$2.3 \cdot 10^{-4}$	$7.9 \cdot 10^{-5}$

[a] Using Nozzle 2 design presented in Table 4 and assuming a wetwell pool of 2000 m^3 and 6 m height.

Micro-scale (injection nozzle): The goal is to confirm that the injection is in turbulent regime, similar to plant case. To achieve this goal, the design parameters needed to be determined are the (i) Reynolds number at injection point. The selection of the design parameters is given below.

(i) The total injection hole area of 64 mm^2 determined in the macro-scale section leads to a nozzle of 9 mm inner diameter. With these dimensions, and using the 1 kg/s flow rate also determined in the macro-scale section, the Reynolds number at the nozzle exit is 1.6e5, which corresponds to a turbulent regime, similar to the one in the BWR presented in Table 4.

The final design of the experiment and nozzle can be observed in Figure 26. Vertical and horizontal injections were achieved by placing a junction in the main pipe. After the junction, a straight pipe of about 200 mm (~200 times the pipe diameter) was used to minimize and flow rotations or inclinations by the junction.

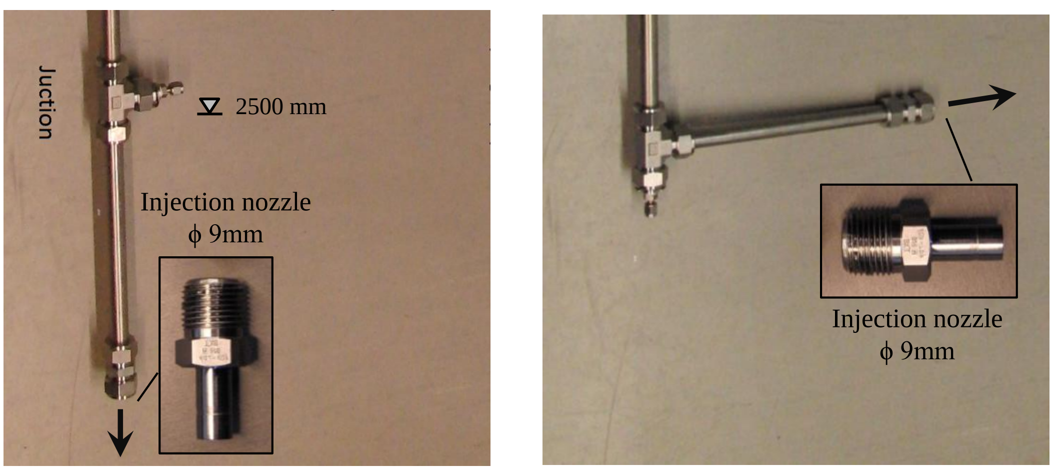

(a) (b)

Figure 26: Mixing nozzles for (a) vertical downwards and (b) horizontal injection PPOOLEX experiments. Images courtesy of operators at PPOOLEX facility, LUT, Finland.

7.2. Pre-test of the nozzle experiments

Pre-test simulations were run using GOTHIC 8.1 (QA) to verify that the scaled nozzle design can induce mixing of the pool. Thermal stratification was first created using sparger, where the EHS/EMS models for spargers presented in section 6.3 were used. After a 20-25 ^{o}C temperature difference was reached between the top and bottom of the pool, the nozzle was activated to induce mixing of the pool.

Due to the axisymmetric flow created by the vertical injection, the simulations were run using a 2D axisymmetric model of the pool, Figure 27. The cell sizes were about 50 mm in the vertical direction and 15 mm in the radial direction. According to the mesh sensitivities done in [99], these values are expected to be fine enough to capture the sharp temperature profiles during the stratification phase created by the sparger, and the jet expansion during the nozzle injection.

The simulations were run using the standard k-Epsilon turbulence model. To avoid unphysical mixing induced by the pool surface, a surface wave damping factor of 60 was used. In the run control parameters, a second order bounded upwind discretization scheme was used in space and a semi-implicit discretization in time. The pressure equation was solved with the conjugate gradient method until a 1e-7 residual was reached after 4 outer implicit loops with 1000 internal iterations each. The minimum time step was set to 1e-7 s and the maximum to 0.08 s

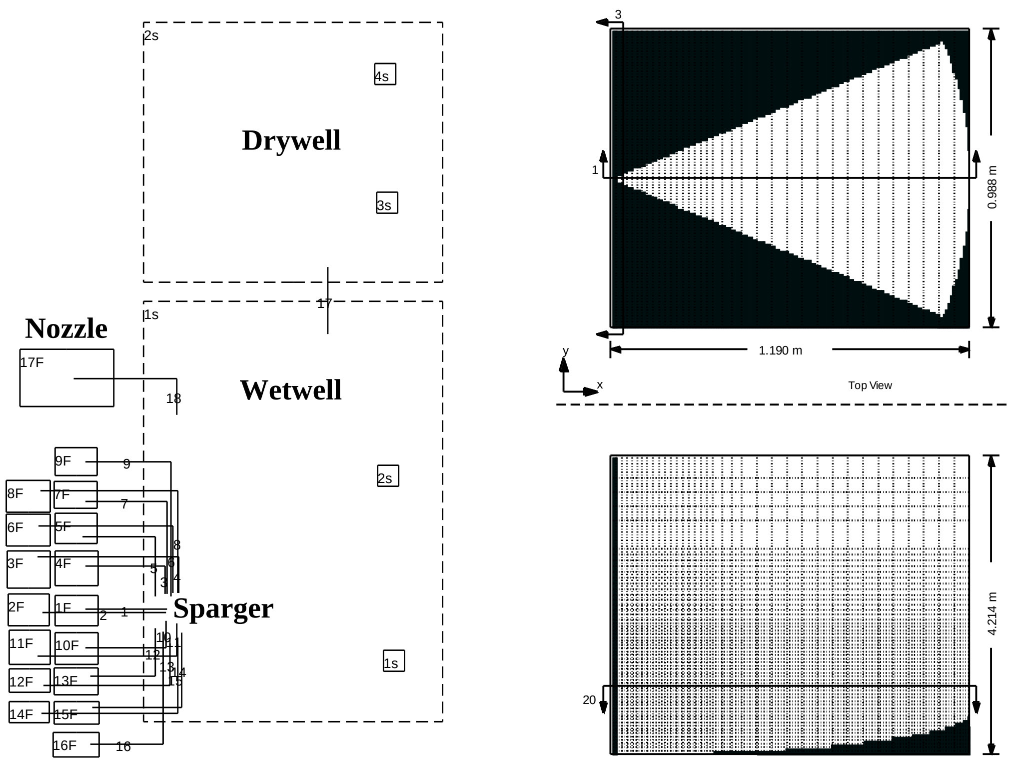

Figure 27: GOTHIC model used during the pre-test nozzle simulations. (a) Control volumes (b) wetwell pool mesh.

The results of the vertical injection are presented in Figure 28 and Figure 30a. It was observed that the 1 kg/s injection determined in the scaling induced a complete mixing of the pool in about 100 s, which is a short transient difficult to use for code validation. Therefore, the flow through the nozzle was reduced to 0.3 kg/s. This flow rate was still able to induce mixing of the pool, but in a much longer time of about 3000 s. The injection temperature through the nozzle was observed to be very influential in the mixing time. We can see in Figure 28a that when the flow was injected at 45 ^{o}C, same temperature as the pool surface, it took about 2000 s more to mix the pool than in the 20 ^{o}C injection, Figure 28b. This is due to the absence of buoyancy forces which would naturally drive down the cold flow injected by the nozzle.

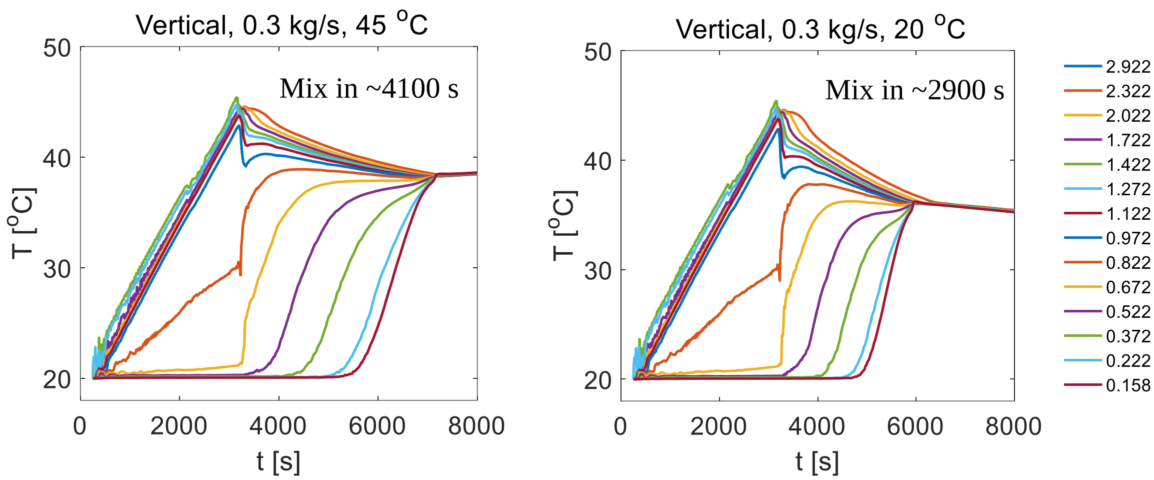

(a) (b)

Figure 28: Pre-test simulations of the PPOOLEX experiments with nozzle. Vertical downwards injection of 0.3 kg/s at (a) 45 °C and (b) 20 °C.

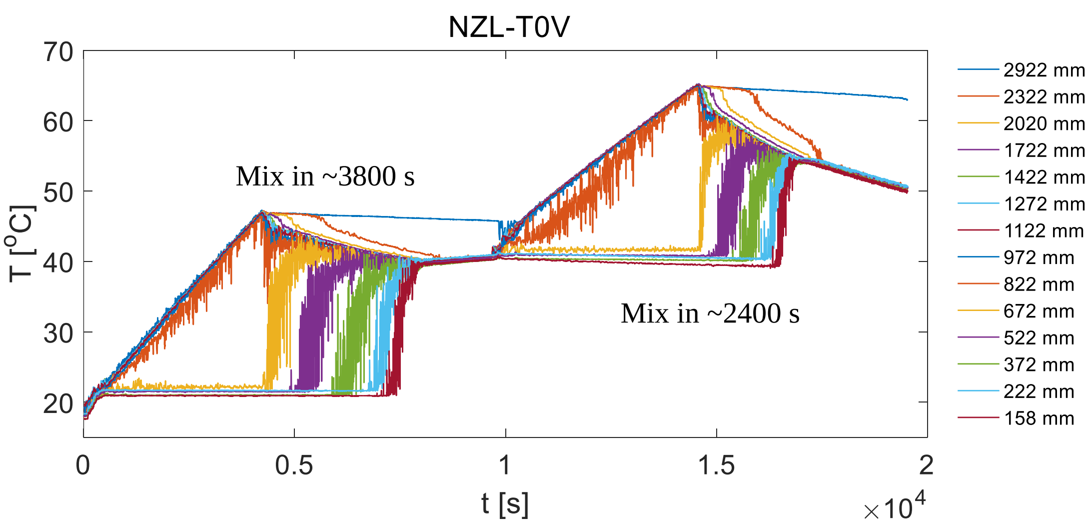

Figure 29: PPOOLEX NZL-T0 experiment. Vertical downwards injection of 0.3 kg/s at 45 °C, mixing phase 1, and 20 °C, mixing phase 2.

Pre-test simulations of the horizontal injection were also carried out. Due to the 3D flow structure induced by the horizontal injection, the simulations were run using a 3D model of the pool. The cell sizes in the vertical direction were maintained at 50 mm, and increased to 120 mm in the horizontal direction. A finer mesh, similar to the one used in 2D, would have been better to capture the jet expansion of the nozzle. However, due to the computational restrictions, such fine mesh could not be afforded.

We can see in Figure 30 that the horizontal injection was much less efficient at mixing the pool than the vertical injection. This is due to the jet impingement on the vessel walls, which reduces the amount of momentum directed downwards, towards the stratified layer. In the vertical case, all of the momentum is directed towards the stratified layer, inducing a much faster mixing.

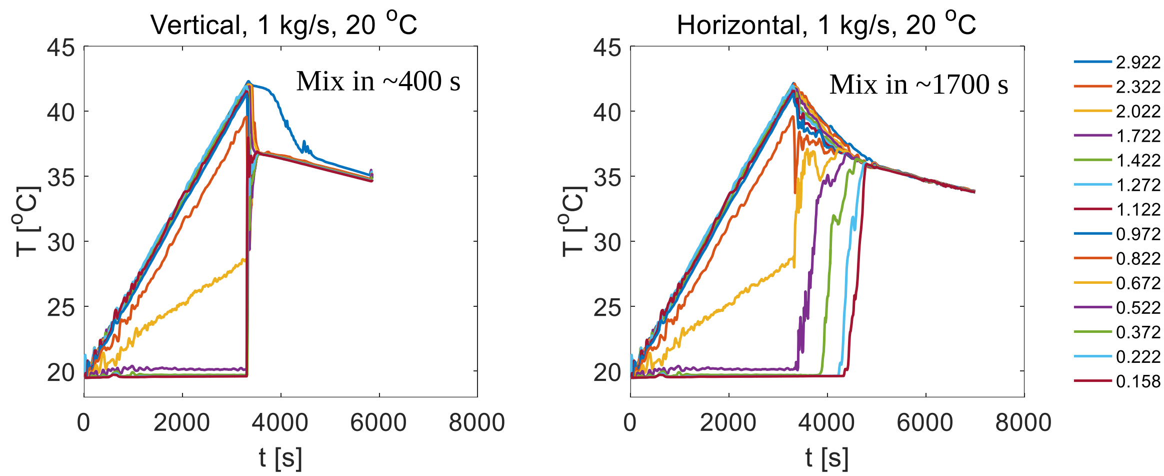

Figure 30: Pre-test simulations of the PPOOLEX experiments with nozzle. (a) Vertical downwards and (b) horizontal injection of 1 kg/s at 20 °C.

The conclusion form the pre-test simulations is that, with the scaled design proposed in section 7.1, the stratified layer can be mixed. The horizontal injection, the one found in the BWRs, was able to induce mixing using the 1 kg/s flow rate determined in the macro-scaling section. The vertical injection, used to allow a more efficient validation, was more efficient in mixing the pool, and the flow rate had to be reduced to 0.3 kg/s in order to have a reasonably long mixing phase.

7.3. PPOOLEX tests with nozzles

Three experiments were performed in the PPOOLEX facility using the scaled nozzle design presented in section 7.1. The goal was to analyze the separate effects of (i) injection temperature, (ii) injection mass flow rate, (iii) temperature difference in the pool, and (iv) orientation of the nozzle. This was achieved through the test-matrix presented in Table 6.

All of the tests began injecting steam at low momentum through the sparger to create a thermally stratified layer. When a certain temperature difference ΔT was reached between the top and bottom of the pool, the nozzle was activated to induce mixing. To analyze the separate effect of the nozzle, the steam injection through the sparger was stopped during the mixing phase. After the first mixing phase, another the stratification-mixing phases were repeated.

The results of the T0V test are presented in Figure 29. This test was designed to study the effect of a different injection temperature through the nozzle. We can see that the mixing phase 1, where water at 45 °C was injected through the nozzle, was about 1.5 times slower than the mixing phase 2, where the temperature was decreased to 20 °C. The mixing times were very similar to the ones predicted in the pre-test simulations, Figure 28. We can also see that the erosion of the stratified layer was very slow. It took about 1 hour to erode 500 mm of the stratified layer.

We can see in Figure 29 that, during the mixing phases, the jet induced by the mixing nozzle was not able to penetrate into the stratified layer. The stepwise temperature increase of the TC measurements located at the bottom of the pool indicate that the stratified layer was slowly eroded at the interface. Moreover, the TCs located at the interface showed low frequency and high amplitude oscillations during this erosion. This is the same behavior as the one observed in the PPOOLEX sparger tests, Figure 14. A Fourier analysis of the temperature measurements located at the interface revealed that there is a leading frequency of about

0.07 Hz, Figure 31. These oscillations are not turbulent since turbulence should have a higher frequency. They were observed to be very similar to the natural oscillation frequencies of the pool, Table 7. Therefore, it was concluded that the pool was excited to this frequency by the action of turbulence. The Brunt–Väisälä frequency, which is the frequency at which a fluid parcel in a stable stratified fluid moves when it is displaced from its stable position, was estimated to be an order of magnitude higher. This is above the acquisition frequency of the TCs. Therefore, it cannot be concluded if this oscillation was also present during the experiment.

Table 6: Test matrix used in the PPOOLEX experiments with nozzle.

NZL series	Nozzle orientation	Stratification phase 1	Mixing phase 1	Stratification phase 2	Mixing phase 2
T0V	Vertical downwards	ΔT = 20 °C [a]	0.3 kg/s [b] 45 °C [b]	ΔT = 20 °C	0.3 kg/s 20 °C
T1V	Vertical downwards	ΔT = 20 °C	0.5 kg/s 45 °C	ΔT = 40 °C	0.3 kg/s 20 °C
T1H	Horizontal	ΔT = 20 °C	1.0 kg/s 20 °C	ΔT = 20 °C	0.3 kg/s 20 °C

[a] Temperature difference between cold stratified layer and the hot region above it
[b] Flow rate and temperature of the liquid injected through the nozzle

Equations (39) and (40) were used to calculate the natural oscillation frequency. It was assumed that the system behaves like a cold pool of depth H with a thermocline separating it from a hot pool above it. With this assumption, H is the stratified layer thickness, R the radius of the tank, k_n the n[th] root of the derivative of the first order Bessel function (k_1 = 1.84, k_2 = 5.33, k_3 = 8.53), and g' the reduced gravity, computed as a function the cold $\rho(T_c)$ and hot $\rho(T_h)$ densities across the thermocline. For the TCs located inside the ellipsoidal cap of the vessel, an equivalent cylinder of radius R with the same volume as ellipsoidal cap below the analyzed TC was used. In the Brunt–Väisälä frequency, equation (41), the density derivative was approximated to a linear density gradient along a thermocline of thickness z_{tc}, which, based on Figure 32, should have a value of about f z_{tc} = 0.1 m. This value derived from the fact that, when the oscillation in a TC reaches its maximum, the TC below does not show any oscillation, thus, z_{tc} < 0.15 m. On the other hand, after the maximum has passed, simultaneous oscillations are observed in the upper and lower TCs, indicating that z_{tc} > 0.075 m. This gives the average value of 0.1 m.

$$f_n = \frac{1}{2\pi}\sqrt{g'\frac{k_n}{R}\tanh\left(H\frac{k_n}{R}\right)} \tag{39}$$

$$g' = g\frac{\rho(T_c) - \rho(T_h)}{\rho(T_c)} \tag{40}$$

$$N = \sqrt{-\frac{g}{\rho}\frac{\partial\rho}{\partial z}} \approx \sqrt{\frac{g'}{z_{tc}}} \tag{41}$$

Fernando et al. [60, 61] demonstrated that, when the momentum forces are small in comparison with buoyancy (large Richardson numbers), the erosion of a stable stratified layer is dominated by the breakup of interfacial waves. This corresponds well to the slow erosion and 0.07 Hz oscillations observed in the PPOOLEX experiments with nozzle. Therefore, the erosion mechanism during these experiments could have been the breakup of the 0.07 Hz oscillations.

Table 7: Comparison between the frequencies observed at the thermocline in the PPOOLEX NZL-T0 experiment, the natural frequencies of the pool, and the Brunt–Väisälä frequencies.

TC location	PPOOLEX NZL-T0V f [Hz]	Natural oscillations f [Hz]	Brunt–Väisälä f [Hz]
0.522 mm	~ **0.067**	ΔT = 40-22 °C, $g' = 0.054$ m/s^2 R = 0.935 m f_1 = **0.045**, f_2 = **0.078** f_3 = **0.098**	$g' = 0.054$ m/s^2 $z_{tc} = 0.1$ m f = **0.73**
0.158 mm	~ **0.076**	ΔT = 38-21 °C, $g' = 0.049$ m/s^2 R = 0.583 m f_1 = **0.043**, f_2 = **0.072** f_3 = **0.092**	$g' = 0.049$ m/s^2 $z_{tc} = 0.1$ m f = **0.70**

It is remarkable how the pre-test simulations provided quite accurate prediction of the results despite the cell size of 15 mm, which is certainly not enough to resolve wave-breaking events. Further analysis needs to be done to clarify the erosion mechanism of the stratified layer.

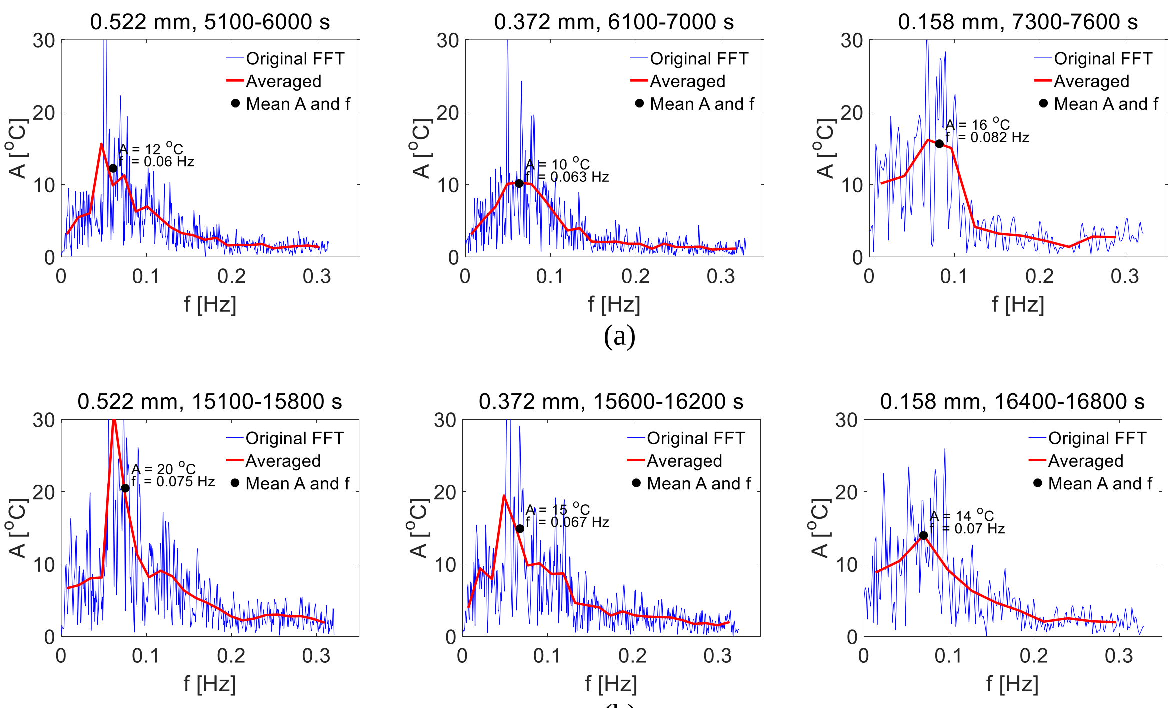

Figure 31: Fast Fourier Transform of the TC measurements from the POOLEX NZL-T0V experiment located at the thermocline during the (a) first and (b) second mixing phases.

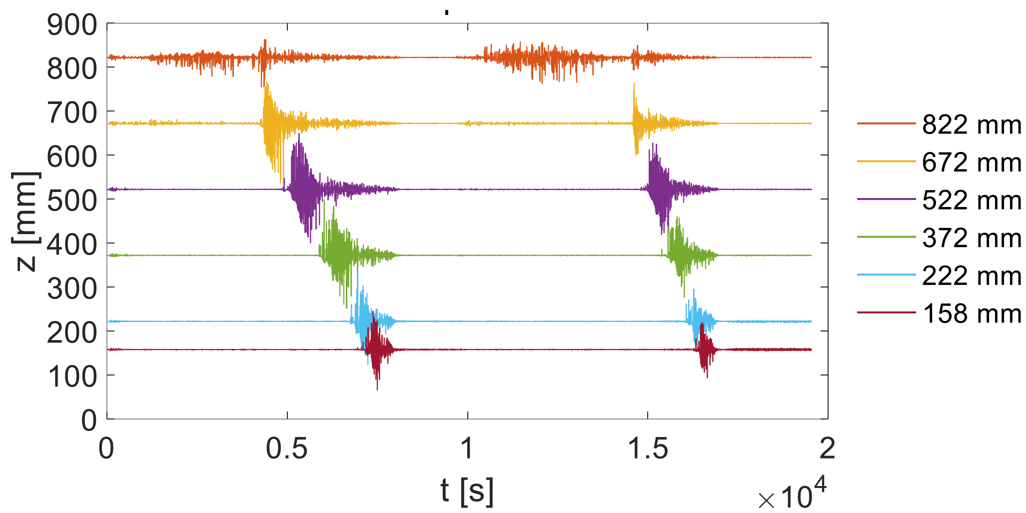

Figure 32: Estimation of the amplitude of the oscillation at the thermocline observed in the POOLEX NZL-T0V experiment.

SUMMARY & CONCLUSIONS

The development of thermal stratification in the pressure suppression pool of BWRs and o the In-containment Refuelling Water Storage Tank (IRWST) of advanced PWRs is a safety issue since it can lead to higher containment pressures than in completely mixed pool conditions, and can affect the operation of the spray and Emergency Core Cooling System (ECCS). The main systems responsible for inducing thermal stratification or mixing of the pool are the spargers, mixing nozzles, blowdown pipes, and sprays. In this work, we have presented the development and validation of Effective Heat Source and Effective Momentum Source (EHS/EMS) models for blowdown pipes, spargers, and mixing nozzles, which enable the prediction of the pool behavior during long term-transients. A summary of the current status on the development and validation of the EHS/EMS models is shown below.

Task-1: To develop EHS/EMS models for the blowdown pipes in case of different steam condensation regimes and presence of non-condensable gases.

In the EHS/EMS models for blowdown pipes, new correlations have been developed to predict the transition between condensation regimes, and to estimate the effective momentum of chugging. These correlations are function of the steam mas flux, pool sub-cooling, and geometry of the injection system. They were built using the PPOOLEX and all other all available experimental data. A new implementation of the EHS/EMS models in GOTHIC has been proposed to enable simulating the pool and containment behavior during prototypic LOCA conditions. A time-averaging model has also been proposed to minimize the effect of the numerical oscillations of the flow in the pool. Validation against the PPOOLEX MIX-04 experiment shows very good agreement to the pool temperatures and containment pressure.

Task-2: To develop EHS/EMS models for spargers and RHR nozzles.

An experimental setup to measure the effective momentum induced by the oscillatory bubble regime during a steam injection through spargers has been designed by KTH and LUT. Preliminary experiments are expected to be performed before the end of the year, and continued through 2018. The experimental data will be used to analyze the physical phenomena affecting the oscillatory bubble regime, and to develop theoretical models which can predict the effective momentum.

Task-3: To provide analytical support for PSP tests in the Nordic BWRs.

A scaling methodology has been developed and applied to the sparger and mixing nozzle experiments performed in PPOOLEX and PANDA. The goal was to preserve prototypical ranges of injection conditions and pool regimes occurring during prototypical BWR transients. The data obtained with the scaled experiments was used for analysis of the physical phenomena and code validation. Important physical phenomena to be considered in the CFD modelling has been identified: for example, the erosion and mixing mechanisms of the stratified layer, the oscillations at the thermocline, the self-similarity of the liquid jets induced by the sparger, and the downwards inclination of the jets. Codes and EHS/EMS models validated for these conditions can be then used to predict plant behavior.

Task-4: To validate the EHS/EMS models against PANDA tests

The EHS/EMS models for sparger have been implemented in ANSYS Fluent. It has been shown that using the k-Omega BSL turbulence model with the SGDH and a $C_{3\varepsilon}$ varying between 0 and 1 allows a good prediction of the stable stratification and erosion regimes. Validation of the EHS/EMS implementation in Fluent against the PANDA HP5-1, 2 experiments shows good agreement with the experimental data.

Task-5: To provide analytical support to NORTHNET partners in addressing containment performance

Further development and validation of the EHS/EMS models will be done against available experimental data to confirm the current hypothesis and further improve the prediction capability. Modelling approaches which allow using the developed EHS/EMS models in coarse mesh models in GOTHIC will also be developed to enable sensitivity and uncertainty analysis of plant transients.

Task-6: Analytical support for PPOOLEX tests and GOTHIC validation

Analytical support has been provided to the PPOOLEX and PANDA experiments with spargers and mixing nozzles. Pre-test simulations were run using GOTHIC. In the mixing nozzle experiments, the experimental results were observed to be very similar to the pre-test predictions. Analytical support will also be given for the separate effect facility to be built in LUT. Post-test analysis of the EHS/EMS models implemented GOTHIC showed good agreement to the pool behavior during the sparger tests SPA T1, T3, T4, T7. However, limitations of the code, mainly the Cartesian mesh, suggested that ANSYS Fluent, where the radial injection of the sparger can be better represented, would be more adequate for this purposes. Therefore, ANSYS Fluent was selected as the computational platform to validate the EHS/EMS models for spargers against the PANDA tests.

ACKNOWLEDGEMENTS

Financial support from the NORTHNET-RM3 and Nordic Nuclear Safety Program (NKS) is greatly acknowledged. The authors are grateful to Markku Puustinen (LUT) and co-workers for very fruitful discussions and unique experimental data which helped a lot in understanding, development and validation of the models. The authors are grateful to all the countries supporting the OECD/NEA HYMERES project and experimental team of PANDA facility lead by Dr. Domenico Paladino, PSI. The authors would like to thank the secretariat and all the members of the Management Board and the Programme Review Group of the HYMERES project for their help in defining the test programme and evaluating the test results.

GOTHIC is developed and maintained by the Numerical Applications Division of Zachry Nuclear Engineering under EPRI sponsorship. We would like to acknowledge NAI for providing access to the program for educational and research purposes.

NKS conveys its gratitude to all organizations and persons who by means of financial support or contributions in kind have made the work presented in this report possible.

DISCLAIMER

REFERENCES

1. Pershagen, B., 1994. Light Water Reactor Safety. Pergamon Press.
2. Y. Zhang, D. Lu, Z. Wang, X. Fu, Q. Cao, 2016. Y. Yang, G. Wu, Experimental research on the thermal stratification criteria and heat transfer model for the multi-holes steam ejection in IRWST of AP1000 plant. Applied Thermal Engineering, 107, 1046-1056.
3. Lahey, R.T., Moody, F.J., 1993. The Thermal Hydraulics of a Boiling Water Nuclear Reactor, 2nd edition, American Nuclear Society, La Grange Park, Ill, USA.
4. Li, H., Kudinov, P., 2010. Effective Approaches to Simulation of Thermal Stratification and Mixing in a Pressure Suppression Pool. OECD/NEA & IAEA Workshop CFD4NRS-3, Bethesda, MD, USA, September 14-16, 2010.
5. Li, H., Villanueva, W., Kudinov, P., 2014. Approach and Development of Effective Models for Simulation of Thermal Stratification and Mixing Induced by Steam Injection into a Large Pool of Water. Science and Technology of Nuclear Installations, 2014, Article ID 108782, 11 pages.
6. Laine, J., Puustinen, M., Räsänen, A., 2013. PPOOLEX experiments on the dynamics of free water surface in the blowdown pipe. Nordic Nuclear Safety Research, NKS-281.
7. J. Laine, M. Puustinen, A. Räsänen, PPOOLEX Experiments with a Sparger, Nordic Nuclear Safety Research, 2015, NKS-334.
8. Mizokami, S., Yamada, D., Honda, T., Yamauchi, D., Yamanaka, Y., 2016. Unsolved issues related to thermal-hydraulics in the suppression chamber during Fukushima Daiichi accident progressions. Journal of Nuclear Science and Technology, 53, 630-638.
9. Mizokami, S., Yamanaka, Y., Watanabe, M., Honda, T., Fuji, T., Kojima, Y., PAIK, C.Y., Rahn, F., 2013. State of the art MAAP analysis and future improvements on TEPCO Fukushima-Daiichi NPP accident. NURETH-15: The 15th International Topical Meeting on Nuclear Reactor Thermal Hydraulics, Pisa, Italy, May 12-17, paper number 536.
10. Tanskanen, V., Jordan, A., Puustinen, M., Kyrki-Rajamäki, R., 2014. CFD simulation and pattern recognition analysis of the chugging condensation regime. Annals of Nuclear Energy, 66, 133-143.
11. Patel, G., Tanskanen, V., Hujala, E., Hyvärinen, J., 2016. Direct contact condensation modeling in pressure suppression pool system. Nuclear Engineering and Design, Article in Press.
12. Pellegrini, M., Naitoh, M., 2016. Application of two-phase flow DFC to the phenomena expected in Fukushima Daiichi S/C. OECD/NEA & IAEA Workshop CFD4NRS-6.
13. Li, H., Villanueva, W., Puustinen, M., Laine, J., Kudinov, P., 2014. Validation of Effective Models for Simulation of Thermal Stratification and Mixing Induced by Steam Injection into a Large Pool of Water. Science and Technology of Nuclear Installations, 2014, Article ID 752597, 18 pages.
14. C.H. Song, S. Cho, H.Y. Him, Y.Y. Bae, M.K. Chung, Characterization of direct contact condensation of steam jets discharging into a subcooled water, Proceedings of IAEA Technical Committee Meeting, PSI, Villigen, 1998.
15. J. Kerney, G.M. Feath, D.R. Olson. Penetration characteristics of a sub-merged steam jet. AIChE Journal 18(3) (1972) 584-553.
16. S.S. Gulawani, S.K. Dahikar, C.S. Mathpati, J.B. Joshi, M.S. Shah, C.S. RamaPrasad, D.S. Shukla. Analysis of flow pattern and heat transfer in direct contact condensation. Chemical Engineering Science, 64 (2009) 1719-1738.
17. X.Z Wu, J.J. Yan, W.J. Li, D.D. Pan, D.T. Chong, 2009. Experimental study on sonic steam jet condensation in quiescent subcooled water. Chemical Engineering Science, 64 (23), 5002-5012.
18. Y.J. Choo, C.H. Song, PIV measurements of turbulent jet and pool mixing produced by a steam jet discharge in a subcooled pool, Nuclear Engineering and Design 240 (9) (2010) 2215-2224.

19. R.J.E. Van Wissen, K.R.A.M. Schreel, C.W.M Van Der Geld, Particle image velocimetry measurements of a steam-driven confined turbulent water jet, Journal of Fluid Mechanics 530 (2005) 353-368.
20. S.H. Ju, H.C. No, F. Mayinger. Measurement of heat transfer coefficients for direct contact condensation in core makeup tanks using holographic interferometer. Nuclear Engineering and Design 199 (2000) 75-83.
21. Chan, C.K., Lee, C.K.B., 1982. A regime map for direct contact condensation. International Journal of Multiphase Flow, 8, 11-20.
22. M.E. Simpson, C.K. Chan, 1982. Hydrodynamics of a subsonic vapor jet in subcooled liquid. Journal of Heat Transfer, 104 (2), 271-278.
23. S. Fukuda, 1982. Pressure Variations due to Vapor Condensation in Liquid, (II). Journal of the Atomic Energy Society of Japan, 24 (6), 466-474.
24. J. Hong, G.C. Park, S. Cho, C.H. Song. Condensation dynamics of submerged steam jet in subcooled water. International Journal of Multiphase Flow 39 (2012) 66-77.
25. S. Cho, S.Y. Chun, W.P. Baek, Y. Kim, 2004. Effect of multiple holes on the performance of sparger during direct contact condensation. Experimental Thermal and Fluid Science, 28 (6), 629-638.
26. J. Tang, C. Yan, L. Sun, 2015. A study visualizing the collapse of vapor bubbles in a subcooled pool. International Journal of Heat and Mass Transfer, 88, 597-608.
27. I. Aya, H. Nariai, M. Kobayashi, 1980. Pressure and Fluid Oscillations in Vent System due to Steam Condensation, (II) High-Frequency Component of Pressure Oscillations in Vent Tubes under at Chugging and Condensation Oscillation. Journal of Nuclear Science and Technology, 20(3), 213-227.
28. D.H. Youn, K.B Ko, Y.Y. Lee, M.H. Kim, Y.Y. Bae, J.K. Park. The Direct Contact Condensation of Steam in a Pool at Low Mass Flux. Nuclear Science and Technology 40(10) (2003) 881-885.
29. W. Villanueva, H. Li, M. Puustinen, P. Kudinov. Generalization of experimental data on amplitude and frequency of oscillations induced by steam injection into a subcooled pool. Nuclear Engineering and Design 295 (2015) 155-161.
30. E. Aust, D. Seeliger. Pool dynamics and dynamic loads in pressure suppression containment systems. Transactions of the American Nuclear Society 41 (1982) 696-699.
31. I. Aya, H. Nariai, 1987. Boundaries between regimes of pressure oscillations induced by steam condensation in pressure suppression containment. Nuclear Engineering and Design, 99, 31-40.
32. K.S. Liang, P. Griffith, 1994. Experimental and analytical study of direct contact condensation of steam in water, Nuclear Engineering and Design, 147 (3), 425-435.
33. S. Cho, C.H. Song, C.K. Park, S.K. Yang, M.K. Chung. Experimental study on dynamic pressure pulse in direct contact condensation of steam jets discharging into subcooled water. Proceedings of NTHAS98. Korea-Japan symposium on nuclear thermal hydraulics and safety; Pusan (Korea, Republic of), 21-24 Oct 1998, 291-298.
34. A. Petrovic de With, R.K. Calay, G. de With, 2007. Three dimensional condensation regime diagram for direct contact condensation of steam injected into water. International Journal of Heat and Mass Transfer, 50 (9-10), 1762-1770.
35. G. Gregu, M. Takahashi, M. Pellegrini, R. Mereu, Experimental study on steam chugging phenomenon in a vertical sparger, International Journal of Multiphase Flow 88 (2017) 87-98.
36. X.Z. Wu, J.J. Yan, W.J. Li, D.D. Pan, G.Y. Liu, W.J. Li, Condensation regime diagram for supersonic/sonic steam jet in subcooled water, Nuclear Engineering and Design 239 (12) (2009) 3142-3150.
37. F. D'Auria, G.M. Galassi, Scaling of nuclear reactor system thermal-hydraulics, Nuclear Engineering and Design 240 (10) (2010) 3267-3293.
38. MARVIKEN-FSCB-I, Marviken Full Scale Containment Blowdown Experiments Series I (1973).

39. W. Kennedy, D. McGovern, R. Maraschin, K. Wolfe. Rigid and flexible vent header testing in the quarter scale test facility. Mark I containment program, task 5.3.3. Technical report, General Electric Co., San Jose, CA (USA), 1978. Alternate Energy Division.
40. T.R. McIntyre, M.A. Ross, L.L. Myers. Mark II pressure suppression test program: Phase I tests. Technical report, General Electric Co., San Jose, CA (USA), 1976. Boiling Water Reactor Systems Dept.
41. W.A. Grafton, T.R. McIntyre, M.A. Ross. Mark II pressure suppression test program: Phase II and III tests. Technical report, General Electric Co., San Jose, CA (USA),1977. Boiling Water Reactor Projects Dept.
42. T.R. McIntyre, L.L. Myers, J.E. Torbeck, R.J. Booker. Mark III confirmatory test program: one third scale, three vent air tests. Technical report, General Electric Co., San Jose, Calif. (USA), 1975. Boiling Water Reactor Systems Dept.
43. A.M. Varzaly, W.A. Grafton, H. Chang, M.K. Mitchell. Mark III confirmatory test program: 1/root 3 scale condensation and stratification phenomena, test series 5807. Technical report, General Electric Co., San Jose, Calif. (USA), 1977. Boiling Water Reactor Systems Dept.
44. T.H. Chuang. Mark III one-third area scale submerged structure tests. Technical report, General Electric Co., San Jose, CA (USA), 1977. Boiling Water Reactor Systems Dept.
45. K. Namatame, Y. Kukita, I. Takeshita, Evaluation of primary blowdown flow rate and vent pipe steam mass flux (Tests 00002, 0003, 0004, 1101, 2101, 3101, 3102) - Full-Scale Mark II CRT program Test Evaluation Report No 1, JAERI-M 83-185 (1983).
46. Y. Kukita, I. Takeshita, K. Namatame, M. Kato, K. Moriya, M. Shiba, Statistical evaluation of steam condensation loads in pressure suppression pool (1) – Full-Scale Mark II CRT program. Test Evaluation Report No. 2, JAERI-M 9665 (1981).
47. J. Hart, W.J.M. Slegers, S.L. de Boer, M. Huggenberger, J. Lopez Jimenez, J.L. Munoz-Cobo Gonzalez, F. Reventos Puigjaner. TEPSS-Technology enhancement for passive safety systems. Nuclear Engineering and Design 209 (2001) 243-252.
48. C.D. Walsche, F.D. Cachard. Experimental investigation of condensation and mixing during venting of a steam/non-condensable gas mixture into a pressure suppression pool. Technical report, IAEA Report (1996) 53-61.
49. Y.T. Moon, H.D. Lee, G.C. Park, CFD simulation of a steam jet-induced thermal mixing into a subcooled water pool, Nuclear Engineering and Design 239 (2009) 2849-2863.
50. Y. Zhang, D. Lu, Z. Wang, X. Fu, Q. Cao, Y. Yang, G. Wu, Experimental research on the thermal stratification criteria and heat transfer model for the multi-holes steam ejection in IRWST of AP1000 plant, Applied Thermal Engineering 107 (2106) 1046-1056.
51. J. Laine, M. Puustinen, Condensation Pool Experiments with Steam Using DN200 Blowdown Pipe, Nordic Nuclear Safety Research (2005) NKS-111.
52. J. Laine, M. Puustinen, Thermal stratification experiments with the condensation pool test rig, Nordic Nuclear Safety Research (2006) NKS-117.
53. J. Laine, M. Puustinen, A. Räsänen, PPOOLEX Experiments on Thermal Stratification and Mixing, Nordic Nuclear Safety Research (2009) NKS-198.
54. M. Puustinen, J. Laine, A. Räsänen, Multiple blowdown pipe experiments with the PPOOLEX facility, Nordic Nuclear Safety Research (2011) NKS-241.
55. J. Laine, M. Puustinen, A. Räsänen, PPOOLEX experiments on the dynamics of free water surface in the blowdown pipe, Nordic Nuclear Safety Research (2013) NKS-281.
56. J. Laine, M. Puustinen, A. Räsänen, PPOOLEX Mixing Experiments, Nordic Nuclear Safety Research, (2014) NKS-309.

57. M. Solom, K.V. Kirkland, Experimental investigation of BWR Suppression Pool stratification during RCIC system operation, Nuclear Engineering and Design 310 (2016) 564-569.
58. D. Song, N. Erkan, B. Jo, K. Okamoto, Dimensional analysis of thermal stratification in a suppression pool, International Journal of Multiphase Flow 66 (2104) 92-100.
59. H.J.S. Fernando, Turbulent mixing in stratified fluids, Annual Review of Fluid Mechanics 23 (1991) 455-93.
60. H.J.S. Fernando, J.C.R. Hunt, Turbulence, waves and mixing at shear-free density interfaces. Part 1. A theoretical model, Journal of Fluid Mechanics 347 (1997) 197-234.
61. J.L. McGrath, H.J.S. Fernando, J.C.R Hunt, Turbulence, waves and mixing at shear-free density interfaces. Part 2. Laboratory experiments, Journal of Fluid Mechanics 347 (1997) 235-261.
62. C.H. Chen, V.K. Dhir. Hydrodynamics of a bubble formed at vent pipe exit. International Journal of Multiphase Flow 8(2) (1982) 147-163.
63. F. Yuan, D. Chong, Q. Zhao, W. Chen, J. Yan, Pressure oscillation of submerged steam condensation in condensation oscillation regime, International Journal of Heat and Mass Transfer 98 (2016) 193-203.
64. J.H. Pitts, Steam chugging in a boiling water reactor pressure-suppression system, International Journal of Multiphase Flow 6 (1980) 329-344.
65. M. Ali, V. Verma, A.K. Ghosh, Analytical thermal hydraulic model for steam chugging phenomenon, Nuclear Engineering and Design 237(19) (2007) 2025-2039.
66. C. Brennen, A Linear Dynamic Analysis of Vent Condensation Stability, Annual Meeting of the American Society of Mechanical Engineers, Chicago, Illinois, November 16-21, 1980.
67. T.J.H. Pättikangas, J. Niemi, J. Laine, M. Puustinen, H. Purhonen. CFD modelling of condensation of vapor in the pressurized PPOOLEX facility. CFD4NRS-3, 14-16 September 2010, Washington D.C., USA.
68. V. Tanskanen, A. Jordan, M. Puustinen, R. Kyrki-Rajamäki. CFD simulation and pattern recognition analysis of the chugging condensation regime. Annals of Nuclear Energy 66 (2014) 133-143.
69. G. Patel. Computational fluid dynamics analysis of steam condensation in nuclear power plant applications. Doctoral dissertation at Lappeenranta University of Technology, Finland, 2017.
70. M. Pellegrini, M. Naitoh, Application of two-phase flow DFC to the phenomena expected in Fukushima Daiichi S/C. OECD/NEA & IAEA Workshop CFD4NRS-6, 2016.
71. H.S. Kang, C.H. Song, CFD analysis for thermal mixing in a subcooled water tank under a high steam mass flux discharge condition", Nuclear Engineering and Design, 238 (2008) 492-501.
72. H.S. Kang, C.H. Song, CFD analysis of a turbulent jet behavior induced by a steam jet discharge through a single hole in a subcooled water tank, Nuclear Engineering and Design, 240 (2010) 2160-2168.
73. R.E. Gamble, T.T. Nguyen, B.S. Shiralkar, P.F. Peterson, R. Greifc, H. Tabatad, Pressure suppression pool mixing in passive advanced BWR plants, Nuclear Engineering and Design 204 (1-3) (2001) 321-336).
74. GOTHIC Thermal Hydraulic Analysis Package, Version 8.1(QA). EPRI, Palo Alto, CA: 2014.
75. RELAP5/MOD3.3 Code Manual Volume IV. US Nuclear Regulatory Commission, Washington DC, 2006.
76. B.L. Smith, G.S. Swift. A comparison between synthetic jets and continuous jets. Experiments in Fluids 34 (2003) 467-472.
77. H. Li, W. Villanueva, P. Kudinov. Effective Models for Simulation of Thermal Stratification and Mixing Induced by Steam Injection into a Large Pool of Water. Nordic Nuclear Safety Research, NKS-316 (2014).
78. I. Aya, H. Nariai. Chugging Phenomenon Induced by Steam condensation into pool water (amplitude and frequency of fluid oscillation). Translated from: Transactions of the Japan Society of Mechanical-Engineers 50 (1984) 2427-2435.

79. C.E. Brennen. Fundamentals of Multiphase Flow. Cambridge University Press (2005), section 15.6.3.
80. J.H. Pitts, Steam chugging in a boiling water reactor pressure-suppression system, International Journal of Multiphase Flow 6 (4) (1980) 329-344.
81. C.K.B Lee, C.K. Chan, Steam chugging in pressure suppression containment: final report July 1976 - July 1979, US Nuclear Regulatory Commission (1980).
82. I. Gallego-Marcos, W. Villanueva, P. Kudinov. Possibility of Air Ingress into a BWR Containment during a LOCA in case of Activation of Containment Venting System. NUTHOS-10: The 10th International Topical Meeting on Nuclear Reactor Thermal Hydraulics, Operation and Safety, Okinawa, Japan, December 14-18, (2014) paper number 1292.
83. I. Gallego-Marcos, W. Villanueva, P. Kudinov. Modeling of Thermal Stratification and Mixing in a Pressure Suppression Pool Using GOTHIC. NUTHOS-11: The 11th International Topical Meeting on Nuclear Reactor Thermal Hydraulics, Operation and Safety, Gyeongju, Korea, October 9-13 (2016) paper number N11P0524.
84. F. D'Auria, G.M. Galassi, Scaling of nuclear reactor system thermal-hydraulics, Nuclear Engineering and Design 240 (10) (2010) 3267-3293.
85. I. Gallego-Marcos, W. Villanueva, R. Kapulla, S. Paranjape, D. Paladino, P. Kudinov. Modeling of thermal stratification and mixing induced by steam injection through spargers into a large water pool. OECD/NEA & IAEA Workshop CFD4NRS-6, Cambridge, MA, USA, September 13-15, 2016.
86. A.A. Sonin. Scaling laws for small-scale modeling of steam relief into water pools, Nuclear Engineering and Design 65 (1) (1981) 17-21.
87. X. Li, M. Zhang, Z. Du, X. Fu. Scaling analysis of coolant spraying process in automatic depressurized system, Annals of Nuclear Energy 72 (2014) 350-357.
88. N.W.M. Ko, K.K. Lau, Flow structures in initial region of two interacting parallel plane jets, Experimental Thermal and Fluid Science 2 (4) (1989) 431-449.
89. D. Heinze, T. Schulenberg, L. Behnke. A Physically Based, One-Dimensional Two-Fluid Model for Direct Contact Condensation of Steam Jets Submerged in Subcooled Water. Journal of Nuclear Engineering and Radiation Science, 1(2) (2015) 8 pages.
90. C.H. Song, S. Cho, H.S. Kang. Steam Jet Condensation in a Pool: From Fundamental Understanding to Engineering Scale Analysis. Journal of Heat Transfer, 134(3) (2012) 15 pages.
91. I. Gallego-Marcos, W. Villanueva, P. Kudinov. Thermal Stratification and Mixing in a Large Pool Induced by Operation of Spargers, Nozzles, and Blowdown Pipes, Nordic Nuclear Safety Research (2016) NKS-369.
92. I. Gallego-Marcos, W. Villanueva, R. Kapulla, S. Paranjape, D. Paladino, P. Kudinov. Scaling and CFD Modelling of the Pool Experiments with Spargers Performed in the PANDA Facility. NUTHOS-11: The 11th International Topical Meeting on Nuclear Reactor Thermal Hydraulics, Operation and Safety Gyeongju, Korea, October 9-13, 2016. N11P0670.
93. ANSYS® Academic Research, Release 17.0, ANSYS Fluent Theory Guide, ANSYS, Inc.
94. A.M. Bahari, K. Hejazi. Investigation of Buoyant Parameters of k-ε Turbulence Model in Gravity Stratified Flows. World Academy of Science, Engineering and Technology 55 (2009).
95. J.W. Miles. On the stability of heterogeneous shear flows. Journal Fluid Mechanics 10 (1961) 496-508.
96. H.D. Abarbanel, D.D. Holm, J.E. Marsden, T. Ratiu. Richardson Number Criterion for the Nonlinear Stability of Three-Dimensional Stratified Flow. Physical Review Letters 52 (1984) 2352-2355.
97. I.P.D. De Silva, A. Brandt, L.J. Montenegro, H.J.S. Fernando. Gradient Richardson number measurements in a stratified shear layer. Dynamics of Atmospheres and Oceans 30 (1999) 47-63.
98. P. Van Gastel, J.L. Pelegrí. Estimates of gradient Richardson numbers from vertically smoothed data in the Gulf Stream region. Scientia Marina 68 (4) (2004) 459-482.

99. I. Gallego-Marcos, L. Filich, W. Villanueva, P. Kudinov. Modelling of the Effects of Steam Injection through Spargers on Pool Thermal Stratification and Mixing. Nordic Nuclear Safety Research (2105) NKS-347.

Bibliographic Data Sheet **NKS-393**

Title	Modelling of a Large Water Pool during Operation of Blowdown Pipes, Spargers, and Nozzles
Author(s)	Ignacio Gallego-Marcos, Walter Villanueva, Pavel Kudinov
Affiliation(s)	Division of Nuclear Power Safety, Royal Institute of Technology (KTH), Stockholm, Sweden
ISBN	978-87-7893-481-9
Date	August 2017
Project	NKS-R / COPSAR
No. of pages	59
No. of tables	7
No. of illustrations	32
No. of references	99

Abstract
max. 2000 characters

In a Boiling Water Reactor, steam released from primary coolant system is condensed in the pressure suppression pool. Thermal stratification in the pool affects pressure suppression capacity of the pool. Heat and momentum sources generated by the steam condensation define pool behavior. Direct Contact Condensation (DCC) of steam present a challenge for contemporary modeling tools. In previous work, the Effective Heat Source (EHS) and Effective Momentum Source (EMS) models were proposed to simulate development of thermal stratification or mixing induced by steam injection into a large pool of water. These models are computationally efficient and sufficiently accurate in resolving the effect of DCC phenomena on the large scale pool circulation.

EHS/EMS models for blowdown pipes have been extended to predict the transition between condensation regimes, estimate the effective momentum of chugging, allow capturing non-uniform condensation along the pipe, and modelling the drywell and wetwell during prototypic LOCA conditions. Validation against the POOLEX-MIX 04 experiment shows very good agreement with the pool temperature and containment pressure.

In the spargers, the experimental data has been analyzed to identify the most important physical phenomena to be considered in the CFD modelling. Based on this analysis, EHS/EMS models for spargers have been developed and implemented in ANSYS Fluent, and validated against the PANDA HP5-1 and 2 experiments. Comparison to pool temperature shows good agreement with the model predictions.

Key words: Thermal Stratification, Mixing, Pressure Suppression Pool, Spargers, Mixing Nozzles, Containment, Thermal Hydraulic, GOTHIC, BWR

Available on request from the NKS Secretariat, P.O.Box 49, DK-4000 Roskilde, Denmark.
Phone (+45) 4677 4041, e-mail nks@nks.org, www.nks.org